Published online 18 November 2021

Nucleic Acids Research, 2022, Vol. 50, No. 3 ***e15***
https://doi.org/10.1093/nar/gkab1076

Improved dsDNA recombineering enables versatile multiplex genome engineering of kilobase-scale sequences in diverse bacteria

Xue Wang[1,†], Wentao Zheng[1,†], Haibo Zhou[1], Qiang Tu[1], Ya-Jie Tang[1], A. Francis Stewart[2,*], Youming Zhang[1,*] and Xiaoying Bian[1,*]

[1]Helmholtz International Lab for Anti-Infectives, Shandong University-Helmholtz Institute of Biotechnology, State Key Laboratory of Microbial Technology, Shandong University, Qingdao, Shandong 266237, China and [2]Genomics, Biotechnology Center, Center for Molecular and Cellular Bioengineering, Technische Universität Dresden, Tatzberg 47–51, 01307 Dresden, Germany

Received March 01, 2021; Revised September 23, 2021; Editorial Decision October 18, 2021; Accepted October 22, 2021

ABSTRACT

Recombineering assisted multiplex genome editing generally uses single-stranded oligonucleotides for site directed mutational changes. It has proven highly efficient for functional screens and to optimize microbial cell factories. However, this approach is limited to relatively small mutational changes. Here, we addressed the challenges involved in the use of double-stranded DNA substrates for multiplex genome engineering. Recombineering is mediated by phage single-strand annealing proteins annealing ssDNAs into the replication fork. We apply this insight to facilitate the generation of ssDNA from the dsDNA substrate and to alter the speed of replication by elevating the available deoxynucleoside triphosphate (dNTP) levels. Intracellular dNTP concentration was elevated by ribonucleotide reductase overexpression or dNTP addition to establish double-stranded DNA Recombineering-assisted Multiplex Genome Engineering (dReaMGE), which enables rapid and flexible insertional and deletional mutagenesis at multiple sites on kilobase scales in diverse bacteria without the generation of double-strand breaks or disturbance of the mismatch repair system. dReaMGE can achieve combinatorial genome engineering works, for example, alterations to multiple biosynthetic pathways, multiple promoter or gene insertions, variations of transcriptional regulator combinations, within a few days. dReaMGE adds to the repertoire of bacterial genome engineering to facilitate discovery, functional genomics, strain optimization and directed evolution of microbial cell factories.

INTRODUCTION

The characterization and engineering of bacterial genomes are cornerstones of prokaryotic functional genomics. Precise and efficient genome engineering technologies are required to better understand prokaryotic genetics, and to develop engineered microbial factories for enhanced chemical production or environmental applications. The deletion, replacement and integration of genes or pathways in bacterial genomes facilitates access to the vast potential offered by engineering prokaryotes (1–3). Multiplex genome editing has been developed to modify multiple genomic loci in parallel and to accelerate the functional selection of combinatorial genomic diversity through directed evolution. Two key technologies, recombineering and CRISPR-Cas (clustered regularly interspaced short palindromic repeats) have been applied in bacteria for multiplex applications to promote strain engineering for functional genomics and industrially significant biomanufacturing (4–15).

Recombineering utilizes phage proteins, originally RecE/RecT from Rac prophage and Redα/Redβ from λ phage (16–18), to promote homologous recombination (HR) for recombinant DNA or bacterial genome engineering (16–22). Recombineering is convenient because phage single strand annealing proteins (SSAPs; most often Redβ) mediate HR between very short regions of sequence identity (16,23,24). These short regions can be easily included in synthetic oligonucleotides, thereby allowing precise, convenient and high throughput design for recombineering exercises. Utilizing oligonucleotide pools, recombineering was applied to multiplex bacterial

*To whom correspondence should be addressed. Tel: +86 532 67721928; Fax: +86 532 58631501; Email: bianxiaoying@sdu.edu.cn
Correspondence may also be addressed to Youming Zhang. Tel: +86 532 67721918; Fax: +86 532 58631501; Email: zhangyouming@sdu.edu.cn
Correspondence may also be addressed to Adrian Francis Stewart. Tel: +49 351 46340129; Email: francis.stewart@tu-dresden.de
†The authors wish it to be known that, in their opinion, the first two authors should be regarded as joint First Authors.

genome engineering to pioneer a new dimension in drive and selection for designated characteristics, including multiplex automated genome engineering (MAGE), trackable multiplex recombineering (TRMR), directed evolution with random genomic mutations (DIvERGE) and pORTMAGE (4–9,25–27).

Recombineering occurs during DNA replication at the replication fork when the phage SSAP anneals single stranded DNA (ssDNA) onto the transiently exposed single stranded DNA template (28,29). Consequently, recombineering does not involve the generation of double strand breaks (DSBs). Phage SSAPs like Redβ do not need their phage partner 5′-3′ exonuclease (like Redα) to mediate HR using single stranded oligonucleotides (23,30). However, a cognate phage pair is required for recombineering with double stranded DNA (dsDNA) (31), because the 5′-3′ exonuclease converts the dsDNA substrate into ssDNA whilst loading the SSAP, which then anneals the ssDNA into the replication fork (32–35).

In contrast to applications with oligonucleotides, multiplex genome engineering with dsDNA has not been developed. Consequently, multiplex applications have only achieved small genome edits so far. Compared to recombineering with oligonucleotides, recombineering with dsDNA offers several advantages, such as the ability to (i) include antibiotic resistance genes for direct selection of small to multi-kilobase engineering tasks; (ii) include complete coding regions, operons or multiple regulatory elements and (iii) utilize PCR to generate multiple substrates.

The CRISPR-Cas system has also been applied for multiplex bacterial applications. CRISPR-Cas9 uses a short guide RNA (gRNA) to introduce a DSB at a target sequence complementary to the gRNA (36–38). The DSB can be repaired by nonhomologous end joining (NHEJ) for site directed mutagenesis or by HR for precise editing. Bacteria primarily utilize HR for DSB repair and have limited, or no, NHEJ repair capability (39). In most bacteria the absence of NHEJ exacerbates the stress and reliance on HR when DSBs are introduced at multiple sites. Consequently, boosting HR by the inclusion of phage recombineering proteins has complemented several CRISPR-Cas9 applications (11–15). Notably, rather than introduce DSBs to stimulate HR as used in eukaryotic applications, Cas9 was first used as a counterselection agent to eliminate parental bacteria that were not mutated by recombineering (11–14). The bacterial inability to cope with DSB challenges emphasizes the utility of alternative CRISPR applications including (i) the use of CRISPR-Cas base editors, which introduce single base changes rather than DSBs (40); (ii) utilizing CRISPR coupled to integrases to mediate RNA guided transpositional insertions (41,42); and (iii) the use of the nuclease-inactivated version of Cas9 to regulate gene expression (although not genome editing, multiplex applications have been described) (43,44).

Redα/Redβ from λ phage works efficiently in *Escherichia coli* and other *Enterobacteriales* as well as several closely related Gram-negative bacteria. For more distantly related bacteria, the Red operon is inefficient and host specific interactions are implicated. To expand the application of recombineering, host-specific recombinase pairs have been identified (45,46) including Redα/Redβ7029 from *Schlegelella brevitalea* DSM 7029, which also performs well in several Burkholderiales strains and the λ Red-like BAS operon from *Pseudomonas aeruginosa* phage Ab31 for *Pseudomonas* species (47–50). Interestingly, we recently reported that phage encoded ssDNA binding (SSB) proteins may expand the recombineering host range (50).

Amongst the drive to extend the technological repertoire for prokaryotic genome engineering, here we address the absence of multiplex dsDNA recombineering. We aimed to develop the multiplex potential of dsDNA recombineering for multiple kilobase-scale sequence replacements, deletions and insertions, which are difficult tasks for ssDNA recombineering. Utilizing comparable experiments in *E. coli, S. brevitalea* and *P. putida,* we identified and optimized protocols that enable multiplex dsDNA recombineering in five diverse bacteria. Our findings have broad implications for prokaryotic genome engineering.

MATERIALS AND METHODS

Strains, plasmids and mutants

All bacteria strains, plasmids, and mutants are described in Supplementary Table S1.

Construction of plasmids and use of Cre/loxM

Synthetic oligonucleotides were purchased from Tsingke Biological Technology and Sangon Biotech and are described in Supplementary Table S2. pR6K-loxM-genta was used as the template for the experiments using gentamicin resistance. The loxM sites are heterotypic lox sites with different spacers (51) and are listed at the bottom of Table S3. We utilized these heterotypic lox sites to enable Cre-mediated deletion of the selectable gene (usually the gentamicin resistance gene) so that it can be re-used for subsequent mutagenesis without Cre-mediated genome rearrangements between the lox sites.

RK2-BAD-Cas9-genta. The oriV (origin of replication) and *trfA* gene were amplified from RK2-apra-cm with primers rk2-5/rk2-3; the inducible promoter P_{BAD} was amplified from pSC101-BAD-ETgA-tet with primers rk2-BAD-5/rk2-BAD-3; the *Cas9* gene was synthesized by BGI (Supplementary Table S3) and the gentamicin resistance gene was amplified from R6K-loxM-genta with primers rk2-genta-5/rk2-genta-3. These four fragments were co-transformed into GB05-dir (22,52) induced for the expression of full length RecE/RecT and selected on LB plates containing 15 μg/ml gentamicin (37°C) for linear plus linear homologous recombination (LLHR) (22) to assemble RK2-BAD-Cas9-genta.

pSC101-HA-cm-HA-gRNA-tet. CREATE cassette plasmids utilize the pSC101 origin and the tetracycline resistance gene. The plasmids were constructed in GB05-dir by LLHR. For example, the pSC101 origin and the tetracycline resistance gene was amplified from pSC101-BAD-ETgA-tet with primers tracRNA-psc101-tet-5/tracRNA-psc101-tet-3; the homology arm HA region (HA-cm-HA) was amplified from R6K-cm-ccdB with primers a-sgRNA-cm-5/a-sgRNA-cm-3; the guide RNA cassette was synthesized

by BGI (Supplementary Table S3). These three fragments were co-transformed into GB05-dir to construct pSC101-HA(A)-cm-HA-gRNA-tet by LLHR.

loxM-cm-ter-GFP-sacB cassette. The loxM-cm-ter-GFP-sacB cassette was made by overlapping PCR using RK2-apra-cm, RK2-Cre-sacB-apra and pBBR1-Rha-GFP-kan as templates. First, the *cm* fragment was amplified from RK2-apra-cm with primers cm-5/cm-3-HA-GFP, GFP fragment was amplified from pBBR1-Rha-GFP-kan with primers GFP-3/GFP-5 while *sacB* fragment was amplified from RK2-Cre-sacB-apra with primers sacB-3/sacB-5-HA-GFP, there were identical regions between these three fragments and the cm-ter-GFP-sacB cassette were obtained with primers cm-5/sacB-3 using above three kinds of fragments as templates, then different loxM-cm-ter-GFP-sacB fragments were obtained by PCR using cm-ter-GFP-sacB as template with different loxM-cm-ter-GFP-sacB-3/loxM-cm-ter-GFP-sacB-3 primer pairs.

Culture conditions

Schlegelella brevitalea DSM 7029 (53), *Paraburkholderia megapolitana* DSM 23488 and their mutants were cultured in CYMG (8 g/l casein peptone, 4 g/l yeast extract, 4.06 g/l $MgCl_2{\cdot}2H_2O$, 10 ml/l glycerin) broth or agar plates with apramycin (20 μg/ml), kanamycin (20 μg/ml) or gentamicin (15 μg/ml) as required. *E. coli* GB2005, *Pseudomonas putida* KT2440, *Pseudomonas syringae* DC3000 and their mutants were cultured in Luria-Bertani (LB) broth or on LB agar plates (1.2% agar) with ampicillin (100 μg/ml), kanamycin (15 μg/ml), chloramphenicol (15 μg/ml) or gentamicin (5 μg/ml) as required. Reagents were purchased from New England Biolabs, Thermo Fisher Scientific, Invitrogen and Sigma-Aldrich.

Asymmetric phosphorothioate dsDNA substrates

The two primers used for PCR synthesis of the dsDNA substrates differed according to the known direction of replication. The primer for the strand that will anneal to the lagging strand template (and consequently serve as a primer for Okazaki-fragment synthesis) was ordered to include two consecutive phosphorothioate (S) bonds at the 5′ end. The primer for the complementary strand was ordered with a 5′ phosphate. Except for the experiment of Figure 1D (before optimization), all cassettes were amplified to establish asymmetrically phosphorothioated dsDNA substrates. All HAs were 100 bp and the primers are listed in Supplementary Table S2.

Multiplex genomic engineering

Original condition for simultaneous glidobactin BGC and BGC7 inactivation in DSM 7029. For *S. brevitalea* DSM 7029 carrying pBBR1-Rha-Redγ-Redαβ7029-kan, the overnight cultures were transferred into 1.3 ml of fresh CYMG liquid medium containing 15 μg/ml kanamycin (starting OD_{600} values were approximately 0.15), and incubated at 30°C, 950 rpm for 14–16 h (the OD_{600} values before induction were ∼1.5), then L-rhamnose was added to induce the expression of the recombinase operon for 90 min. After centrifugation at 9600 rpm for 30 s at room-temperature, the pellet was resuspended in 1 ml of room temperature (RT) ddH_2O. This step was repeated once and the resulting pellet was resuspended in 30 μl RT ddH_2O and immediately electroporated with 1.5 μg dsDNA substrates consisting of equal amounts of gentamicin resistance genes flanked by HAs that either target region A or region B using an Eppendorf 2510 electroporator at 1250 V, and 1 mm gap width electroporation cuvettes. Electroporated cells were incubated in 1 ml antibiotic-free CYMG liquid medium for 4 h at 30°C, 950 rpm on an Eppendorf shaking block, then plated onto CYMG plates containing 15 μg/ml gentamicin. After incubation at 30°C for 48 h, surviving colonies were checked by colony PCR.

Two-large region deletions in DSM 7029. The paired deletions (3, 6 and 10 kb) used 2 × 1.0 μg gentamicin resistance gene flanked by HAs to target two regions in DSM 7029 (pBBR1-Rha-Redγ-Redαβ7029-kan). Two-3 kb deletions: *glbC* (2 682 171–2 685 171) or region *BGC7H* (3 182 150–3 185 150); two-6 kb deletions: *glbC* (2 682 171–2 688 171) or region (3 182 150–3 188 150); two-10 kb deletions: *glbC* (2 682 171–2 693 171) or region (3 182 150–3 193 150). Electroporated cells were incubated in 1 ml antibiotic-free CYMG liquid medium for 4 h at 30°C, 950 rpm, then plated onto CYMG plates containing 15 μg/ml gentamicin and incubate at 30°C for 48 h. Twenty four surviving colonies were checked by colony PCR for each biological replicate.

Promotor replacement of glbB *and* glbC *in DSM 7029.* The same methods as above were used with a genta-P_{apra} cassette amplified from R6K-loxM-genta targeted to the promoter regions of *glbB* or g*lbC* (Supplementary Table S4).

Identification and generation of LTTR mutant strains, followed by simultaneous quartet replacement in DSM 7029. Taking work on *Burkholderia thailandensis* E264 (54) as a starting point, we identified the 49 LTTRs (LysR Transcriptional Regulator) in the *S. brevitalea* DSM 7029 genome. They were individually deleted by recombineering in DSM 7029 (pBBR1-Rha-Redγ-Redαβ7029-kan) by inserting a gentamicin cassette using 100 bp HAs.

To target the four chosen LTTRs, the gentamicin resistance gene was amplified using four pairs of asymmetrically phosphorothioated primers (Supplementary Table S2) and then 1.0 μg of each was co-electroporated into DSM 7029 (pBBR1-Rha-Redγ-Redαβ7029-kan) (the OD_{600} values before induction were approximately 1.5) as described above. 48 surviving clones were checked by colony PCR for each biological replicate.

Two-region replacement in E. coli *GB2005.* The cultivation and preparation methods of competent cells of *E. coli* GB2005 (pBBR1-Rha-Redγβα-kan) were the same as previouly described (22). The competent cells of 1.3 ml *E. coli* GB2005 (pBBR1-Rha-Redγβα-kan) (the OD_{600} values before electroporation were ∼0.8) were mixed with 1.0 μg ampicillin or chloramphenicol resistance genes with HAs to target region A (822 527–823 027) and 1.0 μg chloramphenicol resistance gene to target region B (1 382 497–1 382 997) for electroporation using an Eppendorf 2510

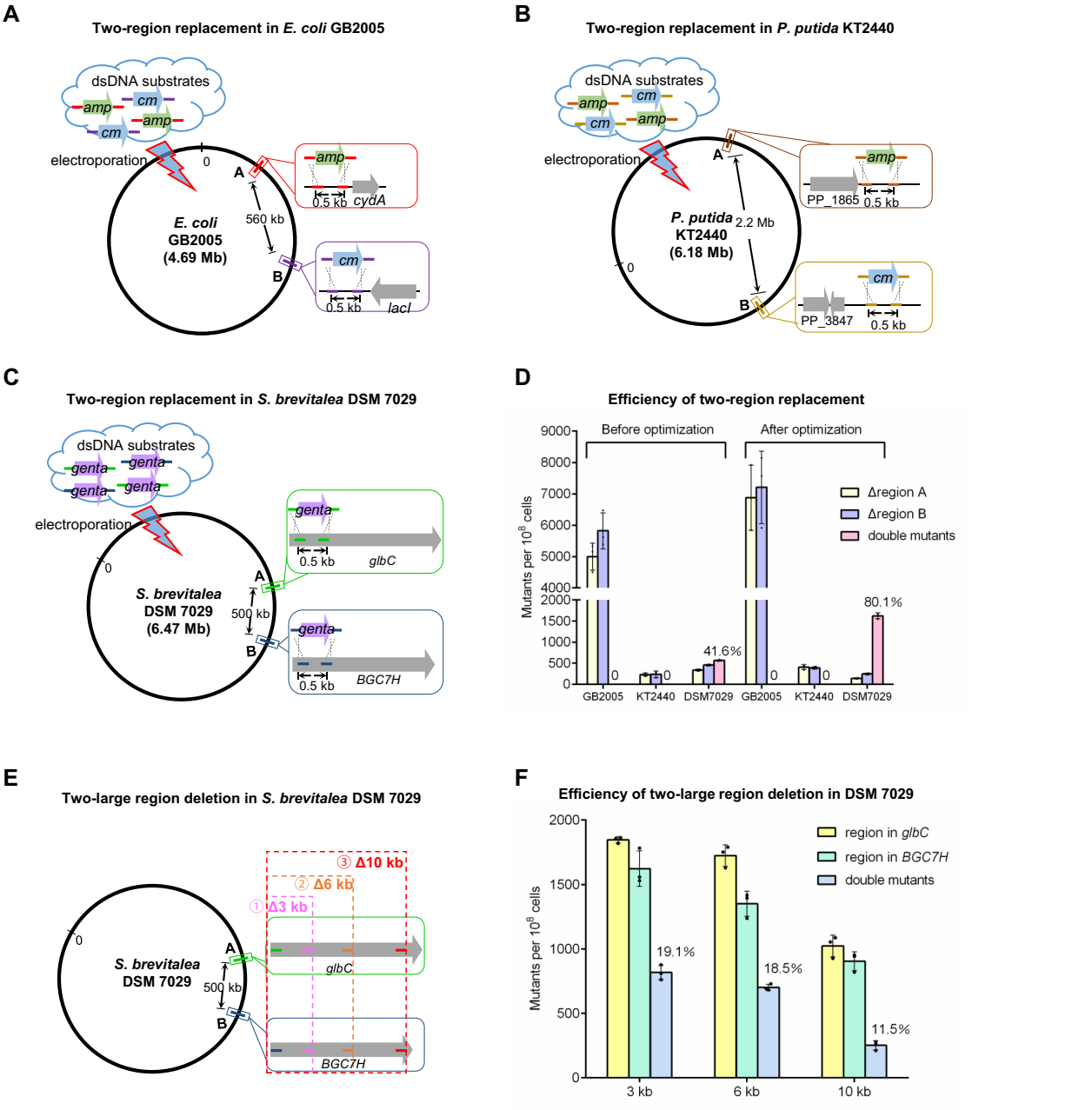

Figure 1. Different performances of dsDNA recombineering-assisted two-region replacement in three bacteria. (**A**) Schematic diagram of dsDNA recombineering assisted two-region replacement in *E. coli* GB2005 (pBBR1-Rha-Redγβα-kan). Region A: 822 527–823 027; region B: 1 382 497–1 382 997. (**B**) Schematic diagram of dsDNA recombineering assisted two-region replacement in *P. putida* KT2440 (pBBR1-Rha-BAS-kan). Region A: 2 087 242–2 087 743; region B: 4 371 516–4 372 016. (**C**) Schematic diagram of dsDNA recombineering assisted two-region replacement in *S. brevitalea* DSM 7029 (pBBR1-Rha-Redγ-Redαβ7029-kan). Region A: *glbC*, AAW51_RS11935, 2 682 171–2 682 671; region B: BGC7 H, AAW51_RS13835, 3 182 150–3 182 650. dsDNA mixtures consisted of resistance genes flanked by pairs of 100 bp HAs were used as illustrated. (**D**) Recombination efficiencies before and after optimization. Δregion A and Δregion B: recombinants with only one region modified. double mutants: mutants with both regions modified. (**E**) Schematic diagram of dsDNA recombineering–assisted two region deletions in DSM 7029. ① Simultaneous deletion of two 3-kb regions. ② Simultaneous deletion of two 6-kb regions. ③ Simultaneous deletion of two 10-kb regions. (**F**) Recombination efficiencies of the experiment illustrated in (E). Values are means of three biological replicates each, where 24 individual surviving clones were assayed per replicate, and the values were normalized to the total number of colonies in each edited sample.

electroporator at 1350 V using 1 mm gap width cuvettes. Electroporated cells were incubated at 30°C in 1 ml antibiotic-free LB liquid medium with or without 10 nM dNTPs (GC50), 950 rpm for 1–12 h before plating (LB, 15 μg/ml chloramphenicol and 50 μg/ml ampicillin) and incubation at 30°C for 12 h. Twenty four clones were checked by colony PCR for each biological replicate.

Six-region replacement of E. coli *GB2005.* As above except that 6.0 × 1.0 μg chloramphenicol resistance genes to target six different target regions (region A–F) were electroporated and 96 surviving clones were checked by colony PCR for each biological replicate. Editing efficiencies were counted as the number of colonies producing all desired replacement junctions from the total number of analysed colonies.

Six-region replacement of E. coli *GB2005 mediated by CREATE.* Firstly, the CREATE-cassettes for regions A-F were built in pSC101 and co-electroporated into *E. coli* GB2005 (pBBR1-Rha-Redγβα-kan). Ninety six surviving clones were checked by colony PCR. Then the plasmid containing arabinose-inducible Cas9 (RK2-BAD-Cas9-genta) was electroporated into the *E. coli* (pBBR1-Rha-Redγβα-kan) with the three CREATE plasmids. In order to avoid cell death caused by leaky Cas9 expression, rhamnose was added to induce the expression of Redγβα recombinase for elevated repair of DSBs. Following electroporation, the cells were recovered in LB, 0.4% rhamnose, 0.4% arabinose at 30°C, with shaking at 950 rpm for 2 h and transferred to a 10× volume LB, 0.4% rhamnose, 0.4% arabinose, 10 μg/ml kanamycin, 4 μg/ml gentamicin, 10 μg/ml chloramphenicol for 37°C overnight recovery. Then, 10 μl overnight culture was transferred into 990 μl LB medium and 100 μl was spread on LB plates, 10 μg/ml kanamycin, 4 μg/ml gentamicin, 10 μg/ml chloramphenicol and incubated at 30°C for 12 h. Clones were picked and double-streaked on LB plates containing either chloramphenicol or tetracycline. Then 96 clones that grew only on the chloramphenicol plate but not tetracycline were selected for colony PCR verification.

Four-4 kb insertions in E. coli *GB2005.* The loxM-cm-ter-GFP-sacB cassette was amplified using four HA pairs and 1.0 μg of each mixed and electroporated into rhamnose-induced GB2005 (pBBR1-Rha-Redγβα-kan). The electroporated cells were incubated in 1 ml antibiotic-free LB liquid medium with or without 10 nM dNTPs (GC50) at 30°C, 950 rpm, for 1–12 h, then plated on to LB plates containing 15 μg/ml chloramphenicol and incubated at 30°C for 12 h. Forty-eight surviving clones were checked by colony PCR for each biological replicate.

Five-BGC knockout in P. megapolitana *DSM 23488. P. megapolitana* DSM 23488 (pBBR1-Rha-Redγ-Redαβ7029-kan) was modified in a similar way as DSM 7029 using the gentamicin resistance gene flanked by 5 HA pairs to target five BGCs (BGC 1, 3, 6, 8, 9) (Supplementary Table S5) using R6K-loxM-genta as PCR template with primers listed in Supplementary Table S2. The electroporated cells were incubated in 1 ml antibiotic-free CYMG liquid medium with or without 10 nM dNTPs (GC50) at 22°C, 950 rpm, for 12 h, then plated on to CYMG plates containing 4 μg/ml gentamicin and incubated at 22°C for 48 h. Ninety-six clones were checked by colony PCR for each biological replicate.

Three-region simultaneous replacement in P. putida. For *P. putida* KT2440 (pBBR1-Rha-BAS-kan), overnight cultures were transferred into 1.3 ml of fresh LB medium containing 15 μg/ml kanamycin, and incubated at 30°C, 950 rpm for 2 h, then L-rhamnose was added to induce the expression of the recombinases for 1 h (the OD_{600} values before electroporation were approximately 0.8). After centrifugation at 9600 rpm for 30 s at room temperature, the pellet was resuspended in 1 ml of room temperature ddH_2O. The wash was repeated and the resulting competent cells were suspended in 30 μl ddH_2O and electroporated (Eppendorf 2510; 1350 V, 1 mm gap width electroporation cuvettes) with 3.0 μg asymmetrically phosphorothioated dsDNA substrates consisting of equal amounts of the gentamicin resistance gene flanked by HAs to target KT2440 region A (2 087 242–2 087 743), region B (4 371 516–4 372 016) or region C (4 372 487–4 372 987). Electroporated cells were incubated in 1 ml antibiotic-free LB liquid medium with 10 nM dNTPs (GC50) for 1 h at 22°C, 950 rpm, then plated on LB plates containing 15 μg/ml gentamicin and incubated at 22°C for 12 h. 24 surviving colonies were checked by colony PCR for each biological replicate.

Three-region simultaneous replacement in P. syringae. *P. syringae* DC3000 (pBBR1-Rha-BAS-kan) was modified in a similar way as *P. putida* KT2440, except the gentamicin resistance gene was flanked by three HA pairs to target region A (1 826 364–1 826 865), region B (4 078 273–4 078 773) and region C (4 079 362–4 079 862) of *P. syringae* DC3000 and electroporated cells of *P. syringae* DC3000 were recovered at 22°C for 4 h and plated on LB plates containing 4 μg/ml gentamicin for 48 h at 22°C.

Spontaneous mutation frequency

The acquisition of rifampicin resistance (Rif^R) by spontaneous mutation was determined as follows: 0.5 μg asymmetrically phosphorothioated HAs to target region A (822 527–823 027) of *E. coli* GB2005 surrounding the chloramphenicol resistance gene were mixed and electroporated into 1.0 ml rhamnose-induced *E. coli* GB2005 (pBBR1-Rha-Redγβα-kan), *E. coli* GB2005-P_{genta}-*nrdAB* (pBBR1-Rha-Redγβα-kan) and *E. coli* GB2005Δ*mutS* (pBBR1-Rha-Redγβα-kan) respectively (the OD_{600} values before induction were adjusted to 0.6). The electroporated cells were incubated in 1 ml antibiotic-free LB with or without 10 nM dNTPs (GC50) at 30°C, 950 rpm, for 1 h. Aliquots (450 μl) were then plated onto rifampicin (100 μg/ml) LB plates for 12 h at 30°C and the colony number was recorded as **S**, or plated (450 μl) onto chloramphenicol (15 μg/ml) LB plates for 12 h at 30°C and the colony number was recorded as **R**, or 100 μl of 10^6 times dilutions were plated onto nonselective LB plates for 12 h at 30°C to determine CFUs with the colony number recorded as **C**. Spontaneous Mutation Frequency (mean value ± SD) was calculated as: 10**S**/0.45**C**, Recombineering efficiency was calculated as: 10**R**/0.45**C** (Supplementary Table S6).

Elimination of selection marker on the genome of DSM 7029 mutants

To remove the antibiotic resistance gene flanked by different loxM sites (Supplementary Table S3), the Cre recombinase expression plasmid, pRK2-BAD-Cre-Apra-sacB, was electroporated and transformants selected in 1.3 ml CYMG medium containing 10 μg/ml kanamycin and 30 μg/ml apramycin at 30°C, 950 rpm for 4 h, followed by 10 μl L-(+)-arabinose (100 mg/ml) to induce the expression of Cre for 4 h at 30°C, 950 rpm. Then 10 μl was transferred into 1.3 ml CYMG medium containing 10 μg/ml kanamycin, 10 μg/ml apramycin and 10 μl L-(+)-arabinose (100 mg/ml) at 30°C, 950 rpm for 4 h, and then this step was repeated. Then 100 μl was spread on CYMG plates containing 10 μg/ml kanamycin and 30 μg/ml apramycin. After 30°C for 36 h, colony PCR confirmed whether the gentamicin selection marker was thoroughly excised from the DSM 7029 genome.

Curing of Cre expression plasmid

To cure the pRK2-BAD-Cre-Apra-sacB, the culture was transferred several times in liquid CYMG medium with increasing concentrations of sucrose. A single colony was inoculated into 1.3 ml CYMG medium with 30 μg/ml kanamycin and 5% sucrose and incubated at 30°C, 950 rpm for 6 h. Then 30 μl was inoculated into 1.3 ml CYMG medium containing 30 μg/ml kanamycin and 7% sucrose at 30°C, 950 rpm for 6 h. Repeat this step but with 10% sucrose, then repeat with 15% sucrose. Plate on 30 μg/ml kanamycin CYMG plates. After incubation at 30°C for 48 h, pick clones for double-streak on CYMG plates (30 μg/ml kanamycin; 10 μg/ml apramycin) and CYMG plates (30 μg/ml kanamycin), respectively. Pick the clones which only grow on kanamycin CYMG plates and verify by colony PCR (primers listed in Supplementary Table S2).

Colony PCR and sequencing

Genomic DNA was isolated by suspending the colony in 1 ml ddH_2O. After heating at 95°C for 15 min, 1 μl boiled sample was used as PCR template. Analytical PCR primers were designed to amplify 0.5–1.5 kb across replacement junctions (Supplementary Table S7), and the PCR products were sequenced with primers (Supplementary Table S2 and Supplementary Figure S25–S36). Editing efficiencies were counted as the number of clones producing all desired replacement junctions from the total number of analyzed clones.

E. coli GB2005 was also sequenced completely and the genome sequence login number in NCBI is PRJNA747614. The genome sequence login number of *E. coli* GB2005Δregion A-F::cm is PRJNA747615.

Fluorescence intensity

The fluorescence cassette consisted of a pair of loxM sites, resistance gene (*cm*), terminator (*ter*), green fluorescent protein reporter gene (*gfp*) and *sacB* counter-selectable gene. The resistance and *gfp* genes are both expressed from the resistance gene promoter. The terminator eliminates unwanted transcription of the *gfp* gene from upstream promoters. To measure fluorescence intensity, cells were plated onto LB, 15 μg/ml chloramphenicol and incubated overnight at 37°C. Colonies were then analyzed by colony PCR to establish GFP copy number. Fluorescence intensity was measured by BioTek Synergy H (Supplementary Table S8).

Real-Time PCR and reverse transcription PCR

E. coli cells from 1.3 ml culture were collected at 12 h (DSM 7029 cells for 24 h). Total RNA was prepared using the RNAprep pure Kit (Tiangen, cat. no. DP430). DNA elimination and reverse transcription was performed with the PrimeScript RT reagent Kit with gDNA Eraser (Takara, cat. no. RR047A). 1 μl cDNA sample was used as real-time PCR template. Real-time PCR was performed on StepOnePlus Real-Time PCR System (Applied Biosystems) using SYBR Premix Ex Taq GC (Takara, cat. no. RR071A) by two-step standard PCR amplification procedure. Oligonucleotides are listed in Supplementary Table S2. The endogenous gene *mdaB*, encoding NADPH quinone reductase (*trxB*, thioredoxin reductase for DSM 7029), was used as the internal control. Expression levels of ribonucleoside diphosphate reductase genes of *E. coli* GB2005 (*glbB* for DSM 7029) were normalized by the expression of the internal control (Supplementary Tables S9 and S10). Data were analyzed using StepOne Software v2.3 (Applied Biosystems).

Western blotting

The endogenous *nrdA* gene was N-terminally tagged with 6× His by recombineering. Western analysis used standard methods. The primary and secondary antibodies were ABclonal Mouse anti His-Tag mAb Cat.No:AE003 and ABclonal AbP71003-D-HRP, respectively, used at 1:1000. The blots were developed with ECL color development kit (GE, RPN2232) and detection with ChemiDoc MP imaging System, Biorad (Supplementary Table S11).

Extraction and analysis of the fermentation extracts

The DSM 7029 wild type strain, 7029::P_{apra}*glbB*, 7029::P_{apra}*glbC* and7029::P_{apra}*glbB*-P_{apra}*glbC* were incubated in 250 ml flasks containing 50 ml CYMG medium plus 10 μg/ml gentamycin unless wt. The culture was inoculated from an overnight culture (the starting OD_{600} value was adjusted to 0.15) with shaking for 48 h at 30°C, 200 rpm. Then resins XAD-16 (2%) were added, and continually incubated for another 48 h. The resin and biomass were harvested by centrifugation and then extracted with 40 ml methanol later. The extracts were concentrated *in vacuo* to dryness and dissolved in 1 ml of methanol before analysis by LC/MS. Standard analysis of crude extracts was measured on an LC-DAD system coupled to a Bruker Impact HD microTOF Q III ESI-MS ion trap instrument operating in positive ionization mode. The chromatographic conditions were: Thermo™ Acclaim™ RSLC 120 C_{18} column, 100 × 2.1 mm, 2.2 μm particle size. Solvent gradient (with solvents A [water and 0.1% of formic acid] and B [acetonitrile and 0.1% of formic acid]) from 5% B at 5 min to 95% B

within 20 min, followed by 5 min with 95% B at a flow rate of 0.3 ml/min. Detection was recorded by both diode array and ESI-MS. The corresponding products of glidobactin BGC were identified by manual comparative metabolic profiles between genta-P_{apra} cassettes addition and wild-type LC/MS chromatograms.

Extraction and purification of Luminmycin F-I (*1-4*)

The overnight 7029::P_{apra}*glbB*-P_{apra}*glbC* culture was incubated 4 l CYMG medium (50 ml × 80) in the presence of 2% XAD-16 resin (added 48 h later) at 30°C for 96 h in shaking flasks (50 ml/250 ml; 200 rpm). The XAD was separated from the supernatant by sieving, washed with 2 l dH_2O twice and extracted with a total volume of 2 l methanol (0.5 l × 4). The resulting extracts (8.66 g) were analyzed by LC/MS, and partitioned with *n*-CH_2Cl_2 and MeOH (3:1) to obtain 0.4 g extracts. The further purification was performed on repeated semi-preparative HPLC instrument equipped with UV detector (210 nm, and 280 nm). A Bruker ZORBAX SB-C18 column (250 × 9.4 mm, 5 μm) was used for further purification with a solvent system consised of water (A) containing 0.1% TFA and acetonitrile (B) containing 0.1% TFA. The gradient was as follows: 0–5 min 60% B, 5–30 min 60–90% B, 30–38 min 90% B, 38–40 min 60% B. Around 6 mg luminmycin F (**1**) was afforded at the retention time of 14.6–15.2 min and 1.5 mg luminmycin H (**3**) at 15.8–16.1 min as white powders. For the NMR data of luminmycin F, see Supplementary Table S12. For the isolation of luminmycin G (**2**) and luminmycin I (**4**), 0.3 g partitioned extracts (CH_2Cl_2: MeOH = 2:1) were further purified by repeated semi-preparative HPLC using the same gradient. Around 5 mg luminmycin G (**3**) was obtained by collection at the retention time of 16.4–16.9 min and 1.2 mg luminmycin I (**4**) at 17.7–18.0 min as white powders. For the NMR data of luminmycin G, see Supplementary Table S13.

Cytotoxicity assay

The cytotoxic effects of luminmycin F-I were determined by MTT assay (55) with human breast cell line MDA-MB-231, human pulmonary carcinoma A549, human hepatocellular line SMMC-7721, human colorectal cell HCT-116, human colorectal adenocarcinoma cells SW480, human chronic myeloid leukemia cells K562, human histiocytic lymphoma cells U937, mouse peritoneal macrophage cells RAW264.7, human hepatocytes LO_2 (Supplementary Table S14).

RESULTS

Recombineering with dsDNA to achieve simultaneous two-region replacement in various bacteria

To determine whether dsDNA recombineering can achieve multiplex engineering in bacterial genomes, we tried simultaneous two-region replacements in *E. coli* GB2005, *P. putida* KT2440 and *S. brevitalea* DSM 7029 using host-specific phage recombinase operons; for *E. coli* GB2005—Redαβγ; for *P. putida* KT2440—BAS; and for *S. brevitalea* DSM 7029—Redβα7029 (17,47–50). Two simultaneous five hundred base pair replacements were attempted in all three hosts (Figure 1A–C). However, success was only achieved in *S. brevitalea* DSM 7029 where 42% of the total picked recombinants were double mutants (7029ΔglbA::genta-ΔBGC7::genta) under gentamicin selection (Figure 1D and Supplementary Figure S1).

Utilizing this success in *S. brevitalea* DSM 7029, we evaluated various parameters including asymmetric 5′ phosphorothioation of the dsDNA substrates. Maresca *et al.* used 5′ phosphorothioated asymmetries on dsDNA substrates to prove that recombineering HR intermediates occur at the replication fork (28). Notably, these 5′ asymmetrically phosphorothioated dsDNA substrates also promoted HR efficiency. We speculated that 5′ asymmetrically phophorothioated dsDNA substrates could also improve simultaneous two-region replacement efficiencies and found a 2-fold improvement (Supplementary Figure S2A). Consequently, we utilized asymmetrically phophorothioated dsDNA substrates, which requires knowledge of the direction of replication so that the 5′ phosphorothioated strand is complementary to the lagging strand template, in all subsequent experiments.

We also varied the densities of competent cells, and the amount and ratio of dsDNA substrates for two-region replacement (Supplementary Figure S2B–D). After optimization of these factors, the efficiency of dsDNA recombineering assisted two-region replacement in DSM 7029 resulted in an optimum of 80% of total picked recombinants (Figure 1D and Supplementary Figure S2D, E).

We then evaluated the ability of dsDNA recombineering for simultaneous deletions at two sites in DSM 7029 under the optimized condition (Figure 1E). Keeping one homology arm (HA) constant and varying the other, either pairs of 3, 6 or 10 kb regions were deleted and the frequency of simultaneous deletion under gentamicin selection ranged between 19.1% and 11.5% (Figure 1F and Supplementary Figure S3).

Notably at this stage we had only achieved two-region replacements in DSM 7029. Despite the optimized approach, we had not observed simultaneous two-region recombineering in either GB2005 or KT2440 even though single-site recombineering in *E. coli* GB2005 was relatively ten-fold higher than in *S. brevitalea* DSM 7029 (Figure 1D). Furthermore, simultaneous two-region recombineering in DSM 7029 was achieved using one selectable gene, gentamicin [*genta*], whereas we employed dual selection (ampicillin [*amp*] and chloramphenicol [*cm*]) in GB2005 and KT2440, which arguably should enhance identification of simultaneous recombineering events. These observations suggested that one or more determinants of simultaneous dsDNA recombineering were present in DSM 7029 but missing in GB2005 and KT2440, which prompted further investigation.

Determinants of dsDNA two-region replacement

The protocols used for the three bacteria differed in several ways including the recovery time after electroporation before selection (which was 4 h for DSM 7029, and 1 h for GB2005 and KT2440), the recovery temperature (which was 30°C for DSM 7029 and KT2440, 37°C for GB2005) and the applied selection (only gentamycin for DSM7029 but both ampicillin and chloramphenicol for GB2005 and KT2440). Consequently, we examined these parameters.

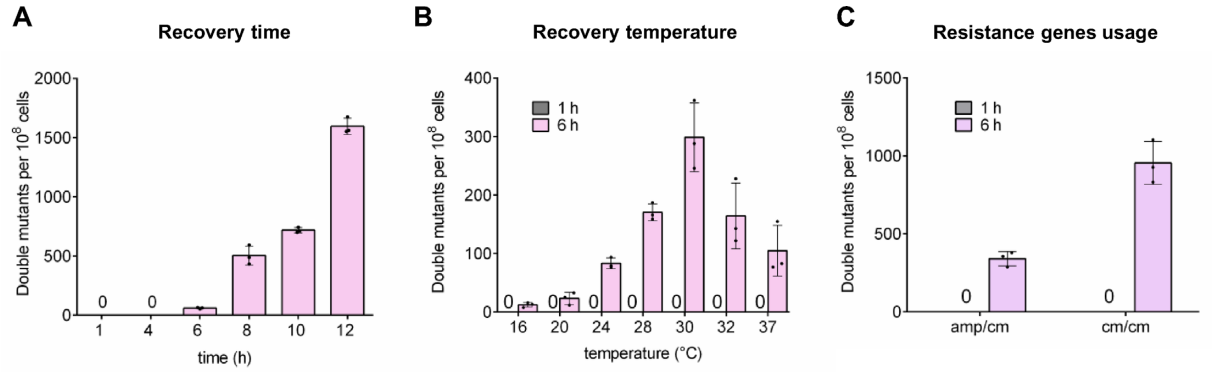

Figure 2. Determinants of dsDNA recombineering-assisted two-region replacement in *E. coli* GB2005 (pBBR1-Rha-Redγβα-kan). (**A**) Efficiency of two-region replacement after different recovery times. (**B**) Efficiency of two-region replacement at different recovery temperatures with 1- or 6-h of recovery. (**C**) Efficiency of two-region replacement selecting for one or two antibiotic resistance genes with 1- or 6-h of 30°C recovery. The resistance genes were flanked by 100 bp HAs; Amp/cm, GB2005 ΔregionA::cm-ΔregionB::amp; cm/cm, GB2005 ΔregionA::cm-ΔregionB::cm. The values are the means of three biological replicates each, where 24 individual surviving colonies were assayed per replicate and were normalized to the total number of clones for each edited sample.

In *E. coli* GB2005, double mutants appeared when the recovery time was extended to 6 h and substantially increased at 12 h (from 60 clones/10^8 cells at 6 h to 720 clones/10^8 cells at 12 h; Figure 2A). The absence of double mutants at 1 h was not changed by reducing the recovery temperature. However, at 6 h recovery time, reduced temperature improved the dual recombineering efficiency with an optimum at 30°C (Figure 2B). This optimum differs from the previously reported *E. coli* recombineering optima of 37°C. We then tested the effects of selection using one [*cm*] or two [*amp* and *cm*] resistance genes. After 6 h recovery at 30°C, dual recombinants were obtained in both cases whereas none had been obtained after 1h recovery. Notably three times more dual recombinants were observed at 6 h using single [*cm*] rather than dual selection (954/10^8 cells versus 340/10^8; Figure 2C). This observation suggests the presence of a subpopulation of proficient hosts capable of multiple recombineering events, which has been previously suggested for ssDNA recombineering and is the basis for CoMAGE (7,8). Alternatively, the use of one resistance gene may be sufficient to select for the cell subpopulation that was most efficiently electroporated and that double selection is deleterious for the selection of this subpopulation. These results indicate that the recovery time and temperature are important determinants for multiplex dsDNA recombineering.

Improved multiplex dsDNA recombineering by increasing available dNTPs

Because dsDNA recombineering occurs at the replication fork (28,29), we reasoned that simultaneous dsDNA recombineering could be enhanced during recovery by altering the speed of the replication fork, which is limited by the intracellular dNTP pool. In *E. coli*, the rate-limiting step in dNTP production is regulated by ribonucleotide reductase (RNR), which catalyzes the reduction of ribonucleotide diphosphate (NDP) to deoxyribonucleoside diphosphate (dNDP) (56). In *E. coli*, the speed of DNA replication is directly related to dNTP levels and RNR overexpression increases the speed of DNA replication fork (57–61). To accelerate the replication fork, we overexpressed RNR and evaluated dual dsDNA recombineering. We replaced the original promoter of the *nrdA*, *nrdB* operon, which encodes RNR, with the strong promoter from the gentamicin resistance gene, P_{genta}, to establish *E. coli* GB2005-P_{genta}-*nrdAB*. The transcriptional level of *nrdAB* was improved five-fold (Supplementary Figure S4A and Table S9), and Western analysis showed that NrdA expression was also strongly elevated (Figure 3A; Supplementary Figure S4B and Table S11). The RNR overexpression strain delivered a striking result. Double dsDNA mutants in *E. coli* GB2005-P_{genta}-*nrdAB* were found after only 1 h of recovery (at 30°C), and at 6 h recovery, the efficiency of two-region replacement was 8.6-fold of that in the GB2005 wild-type strain (1032/10^8 cells versus 120/10^8 cells; Figure 3B).

To support the RNR overexpression experiment and the implication that increased dNTP levels could improve double dsDNA recombineering, we added dNTPs to the recovery buffer reasoning that dNTPs may enter the host during recovery from electroporation. In concordance with RNR overexpression, dual dsDNA recombineering was also promoted by dNTP addition. Added dNTPs ranged from 0.1 to 1000 nM with optima observed at 10 and 20 nM after both 1 and 6 h recovery, including the highest efficiency yet observed (2262/10^8 cells at 6 h; Figure 3C). These results reveal that the addition of moderate amounts of dNTPs in the recovery stage strongly promotes dual dsDNA recombineering in *E. coli*.

Previous reports have shown that increased intracellular dNTP levels lead to increased spontaneous mutation rates (57,59). We used the gain of spontaneous *E. coli* rifampicin resistance to evaluate the spontaneous mutation rate caused by added 10 nM dNTPs. A standard dsDNA recombineering exercise was performed in GB2005 with and without 10nM dNTPs added to the recovery phase. For comparison we included the RNR overexpression strain, GB2005-P_{genta}-*nrdAB* and a mutant mismatch repair strain, GB2005Δ*mutS*::genta. Notably both added dNTPs and elevated RNR expression increased standard recombineering but showed only a small increase in mutagenesis ($\sim 5 \times 10^{-7}$ to $\sim 8 \times 10^{-7}$). Similarly, standard recombineering was elevated in the absence of mismatch repair, however sponta-

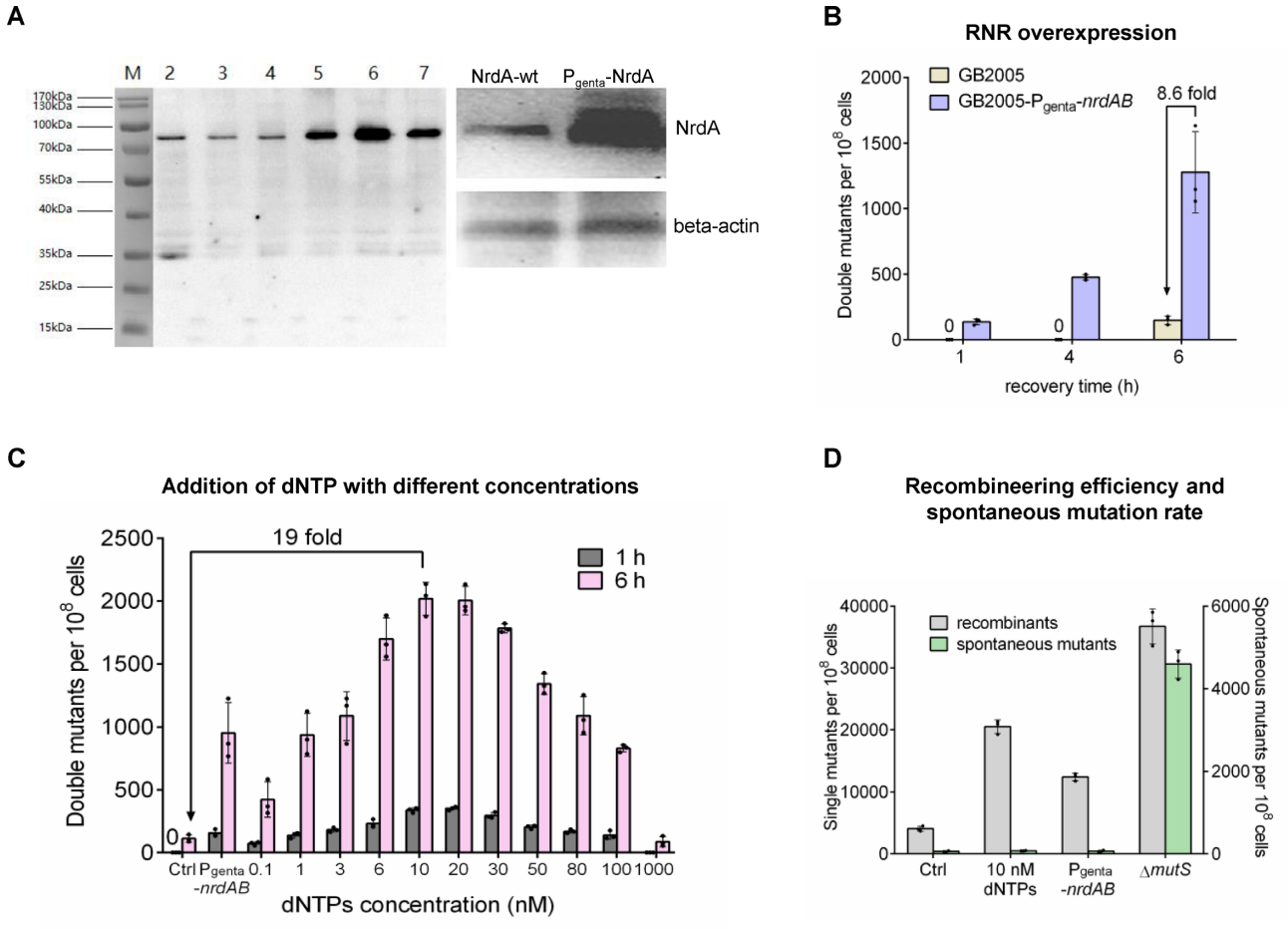

Figure 3. Improved multiplex dsDNA recombineering by increasing available dNTPs. (**A**) Western blot of NrdA expression in *E. coli* GB2005 (lanes 2, 3 and 4) and *E. coli* GB2005-P_{genta}-*nrdAB* (lanes 5, 6 and 7). Inset – overexposure of lanes 4 and 5 with beta-actin loading control. (**B**) Effects of RNR overexpression on dsDNA recombineering-assisted two-region replacement in *E. coli* GB2005 after 1-, 4- or 6-h of 30°C recovery using ΔregionA::amp-ΔregionB::cm as in Figure 2. (**C**) Effect of dNTP concentration on two-region replacement after 1- or 6-h of 30°C recovery as in (B). (**D**) Comparison of spontaneous mutation rates and recombineering efficiencies in *E. coli* GB2005 and mutant derivatives. Ctrl - *E. coli* GB2005; 10 nM dNTPs: *E. coli* GB2005 with added 10 nM dNTPs; P_{genta}-*nrdAB*: *E. coli* GB2005-P_{genta}-*nrdAB*; Δ*mutS*: *E. coli* GB2005Δ*mutS*. The values are the means of three biological replicates each, where 24 individual surviving colonies were assayed per replicate and were normalized to the total number of clones for each edited sample.

neous mutagenesis was also strongly elevated, as expected (Figure 3D).

Multiplex dsDNA recombineering compared to CREATE

To evaluate the impact of elevated dNTPs on multiplex dsDNA recombineering, we aimed to replace six regions (termed A-F) on the *E. coli* genome in one electroporation using only one selectable gene (cm) (Figure 4A). A full spectrum of multiple mutants was generated in a single round at 30°C recovery with asymmetrically phosphorothioated dsDNA substrates and 10 nM dNTPs (Figure 4B and Supplementary Figure S4C and D). Even at 1 h recovery, 2% of chloramphenicol resistant colonies were sextuple mutants, rising to 10% at 12 h recovery. Sextuple mutants were not obtained in *E. coli* GB2005 without dNTP addition even after 12 h of 30°C recovery. In GB2005-P_{genta}-*nrdAB*, sextuple mutants (GB2005-P_{genta}-nrdABΔregionA-F::cm) were obtained after 4 h of 30°C recovery without dNTP addition (Figure 4B).

We used this sextuple mutagenic exercise for a comparison with CRISPR-enabled trackable genome engineering (CREATE), which also can mediate multiplex genome editing of *E. coli* using dsDNA as substrates (13). CREATE-mediated genome editing relies on DSBs generated by Cas9 that are repaired by HR using a cassette flanked by homology arms (HAs) that is excised by Cas9 from a plasmid (Figure 4C and Supplementary Figure S4E). We flanked the chloramphenicol resistance gene with 100 bp HAs for each of the six target regions (region A–F), cloned into the pSC101 temperature-sensitive plasmid that can be eliminated by raising the culture temperature to 37°C. Firstly, we tried to transfer the six plasmids into *E. coli* GB2005 (pBBR1-Rha-Redγβα-kan) simultaneously. However, likely due to the plasmid incompatibility, at most only three different plasmids were obtained per host (Supplementary Figure S4F). Then the Cas9 expression plasmid (RK2-pBAD-Cas9-genta) was electroporated into the host carrying three plasmids (for regions B, D and E). However, after induction and selection, only two-region mutants

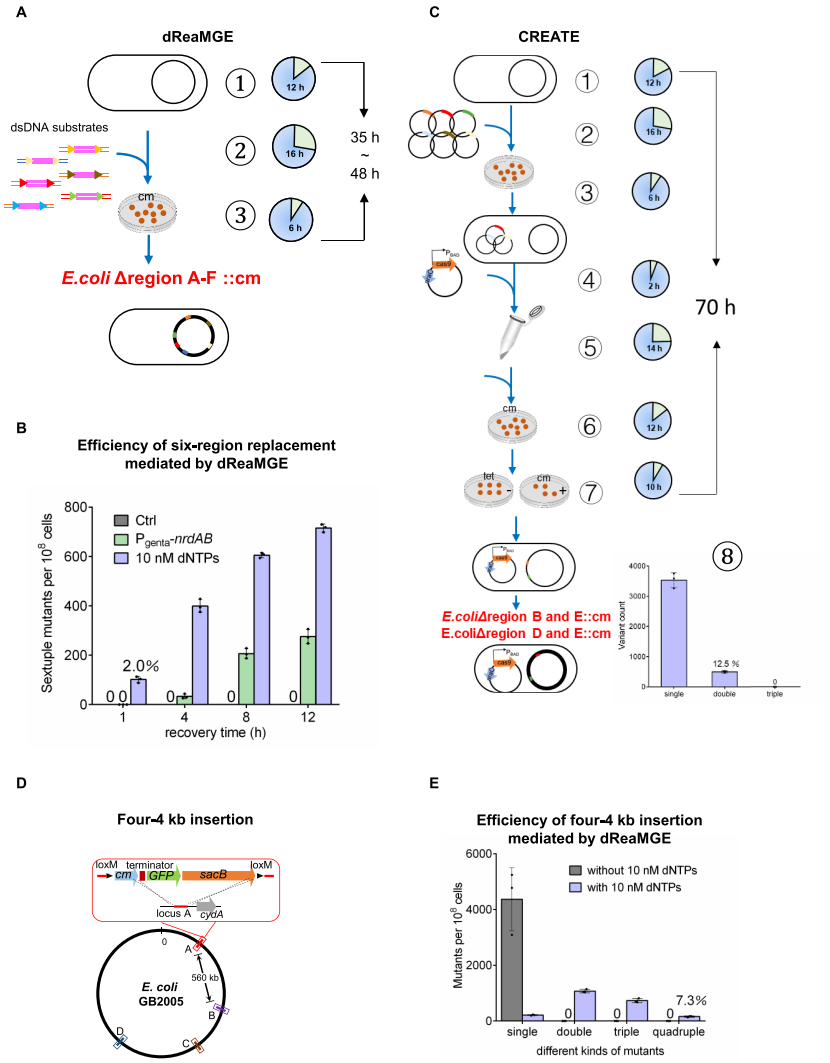

Figure 4. The establishment of dReaMGE in *E. coli* GB2005. (**A**) Schematic workflow of a six-region replacement: ① Cell culture (*E. coli* GB2005 with pBBR1-Rha-Redγβα-kan) with rhamnose induction of the Red operon for the final 40 min–12 h; ② Electroporation of the 6 HA flanked *cm* resistance genes with recovery at 30°C for 1–12 h, spreading on LB plates containing 15 μg/ml chloramphenicol and incubation at 30°C for 12–16 h. ③ Colony PCR – 6 h. (**B**) Efficiency of six-region replacement in *E. coli* GB2005 (pBBR1-Rha-Redγβα-kan) with or without 10 nM dNTP, or *E. coli* GB2005-P_{genta}-*nrdAB* (pBBR1-Rha-Redγβα-kan) for different recovery times at 30°C. (**C**) Schematic workflow of an exercise to use CREATE for a six-region replacement. ① Cell culture (*E. coli* GB2005 with pBBR1-Rha-Redγβα-kan) –12 h. ② Electroporation of the six pSC101 CREATE cassettes into *E. coli* (pBBR1-Rha-Redγβα-kan), recovery and selection –12–16 h. ③ Colony PCR – 6 h. ④ Electroporation of the Cas9 expression vector RK2-pBAD-Cas9-genta into *E. coli* (pBBR1-Rha-Redγβα-kan with three pSC101 CREATE cassettes) and recovery at 30°C – 2 h. ⑤ Cell culture at 37°C – 14 h. ⑥ Plating on LB (kan/genta/cm) and incubation at 30°C for 12 h. ⑦ Replica-streaking on LB (cm or tet), and incubation at 30°C for 6 h, to identify clones that grow only on chloramphenicol and not tetracycline followed by colony PCR verification – 10h. ⑧ The observed outcome efficiency of the CREATE exercise to replace three regions simultaneously. (**D**) Schematic of an exercise to insert four 4-kb cassettes in *E. coli* GB2005 (pBBR1-Rha-Redγβα-kan). (**E**) Efficiencies after 1-h of recovery at 30°C recovery with or without 10 nM dNTPs. The values are the means of three biological replicates each, where 96 individual surviving clones were assayed per replicate, and the values were normalized to the total colony number of clones for each edited sample.

were obtained. In addition to these technical limitations, the CREATE process took at least twice as long to achieve two double mutant combinations (GB2005Δregion B and E::cm and GB2005Δregion D and E::cm; Figure 4C and Supplementary Figure S4G), than the simpler dReaMGE protocol, which generated sextuple mutants.

In a further application, we tested the ability of dReaMGE to mediate multiple kilobase insertions in *E. coli* GB2005. Four pairs of 100 bp HAs were attached by PCR to a 4 kb cassette (including loxM sites flanking the cm gene followed by a terminator [ter] and apramycin promoter driving a GFP-sacB operon; Figure 4D). After co-electroporation and 1 h recovery at 30°C with 10 nM dNTPs, quadruple mutants were obtained in 7.3% of the total picked recombinants under chloramphenicol selection with useful frequencies of double and triple combinations (Figure 4E and Supplementary Figure S5A, B). The fluorescence intensities (FIs) of the insertion mutants containing one to four loxM-cm-ter-GFP-sacB cassettes were measured, yielding a positive linear correlation to the copy number of inserted GFP genes (Supplementary Figure S5C and Supplementary Table S8). Potentially, the four loxM-cm-

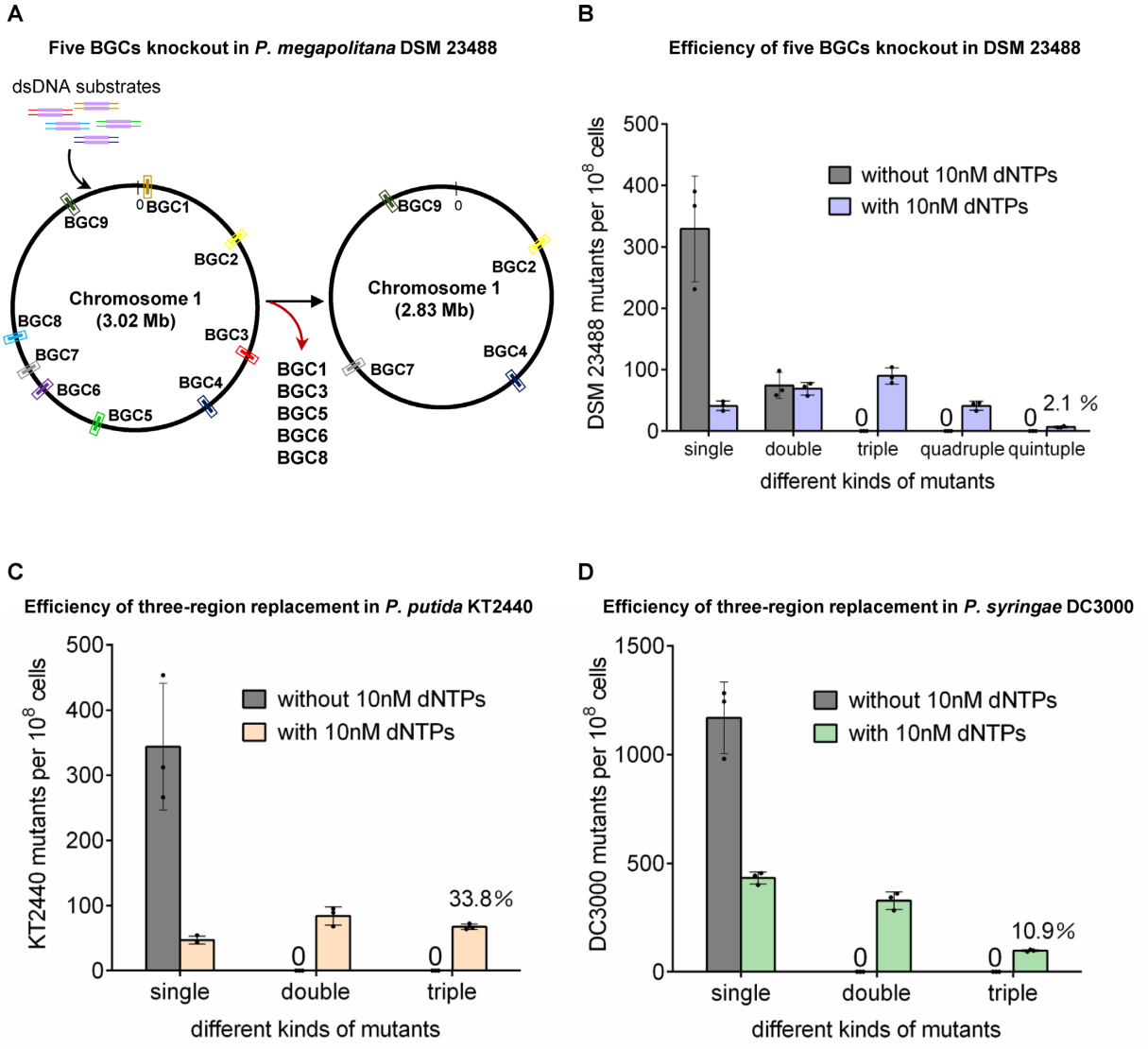

Figure 5. Application of dReaMGE in *P. megapolitana* DSM 23488, *P. putida* KT2440 and *P. syringae* DC3000. (**A**) Schematic of dReaMGE five simultaneous BGC knockouts in *P. megapolitana* DSM 23488 (pBBR1-Rha-Redγ-Redαβ7029-kan). (**B**) Efficiencies after 12-h of recovery at 22°C with or without 10 nM dNTPs. (**C**) Efficiency of dReaMGE three-region replacement in *P. putida* KT2440 (pBBR1-Rha-BAS-kan) under optimal conditions after 1-h of recovery at 22°C with or without 10 nM dNTP. (**D**) Efficiency of dReaMGE three-region replacement in *P. syringae* DC3000 (pBBR1-Rha-BAS-kan) under optimal conditions after 4-h of recovery at 22°C with or without 10 nM dNTPs. The values are the means of three biological replicates each, where 24 clones (96 for B) were assayed per replicate, and the values were normalized to the total number of clones for each edited sample.

ter-GFP-sacB cassettes in the quadruple mutants could be removed using Cre recombinase with or without *sacB* counterselection to remove the inserted genes or to achieve further genome rearrangements (Supplementary Figure S5D).

Application of dReaMGE in diverse bacteria

The elevation of intracellular dNTP concentration combined with the use of asymmetric 5′ phosphorothioates and protocol optimization facilitated multiplex dsDNA genome engineering in *S. brevitalea* DSM 7029 and *E. coli* GB2005, which encouraged us to widen applications to more bacteria.

Previously we developed recombineering for *P. megapolitana* DSM 23488 using Redγ-Redβα7029 (49). For multiplex dsDNA engineering, we prepared gentamicin resistance cassettes to delete five BGCs (Biosynthetic Gene Clusters) in the DSM 23488 genome: BGCs 1 (13 kb), 3 (32 kb), 5 (95 kb), 6 (49 kb) and 8 (11 kb) (Figure 5A and Supplementary Table S5). All five loci are on chromosome 1 and were targeted by a dsDNA mixture consisting of five pairs of 100 bp HAs flanking the *genta* resistance gene using 12 h recovery at 22°C. Notably, 10 nM dNTPs was also optimal for recombineering in *P. megapolitana* DSM 23488 (Supplementary Figure S6A). Of the total checked recombinants, 2.1% were quintuple mutants under gentamycin selection. This new strain, DSM23488Δ5BGCs::genta, was reduced by 200 kb (Figure 5B and 6.3% of chromosome 1 or 2.6% of the entire genome) compared to parental *P. megapolitana* DSM 23488 (Supplementary Figure S6B, C).

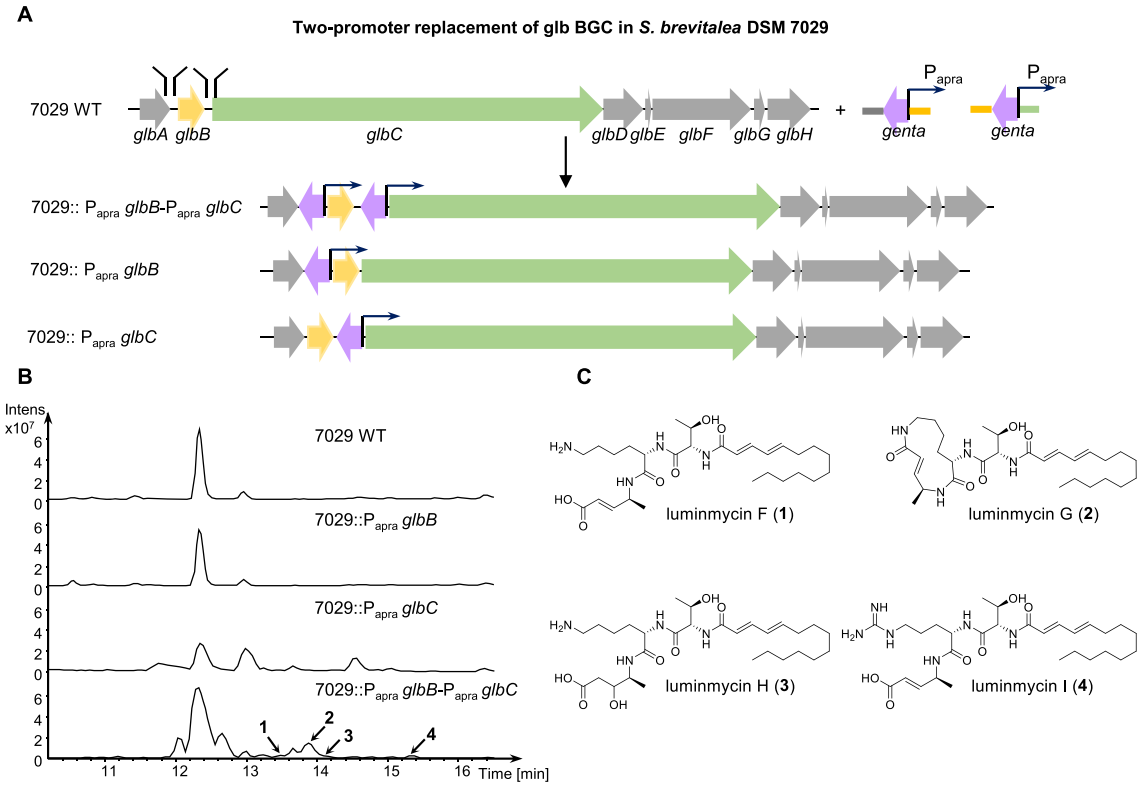

Figure 6. dReaMGE in *S. brevitalea* DSM 7029 (pBBR1-Rha-Redγ-Redαβ7029-kan) for engineering biosynthesis of glidobactin. (**A**) Schematic of dReaMGE simultaneous two-promoter replacement in DSM 7029. The gentamycin resistance gene is shown as a large purple arrow, which indicates its direction of transcription. The P_{apra} promoter is indicated as the thin arrows and the flanking 100 bp HAs are colored corresponding to their insertion sites in the *glb* promoter region. (**B**) LC–MS analysis (BPC + All MS) of DSM 7029 wild-type strain, 7029 P_{apra}*glbB*, 7029 P_{apra}*glbC* and 7029 P_{apra}*glbB* P_{apra}*glbC* (RT = 12–15 min). (**C**) Structures of luminmycins F, G, H and I denoted as **1**–**4**.

For *P. putida* KT2440 and *P. syringae* DC3000, we used the BAS recombinase operon (50) and checked protocol optimization again (Supplementary Figures S7 and S8). Three regions in the KT2440 genome were targeted using 100 bp HAs flanking the *genta* resistance gene and 1 h recovery at 22°C with 10 nM dNTPs. One third (33.8%) of the total picked recombinants were triple mutants (KT2440ΔregionA-C::genta) under gentamicin selection (Figure 5C and Supplementary Figure S7). Triple mutants of DC3000 were obtained through the same procedure as KT2440 with 4 h recovery at 22°C, and 10.9% of the total picked recombinants were found to be DC3000ΔregionA-C::genta under gentamicin selection (Figure 5D and Supplementary Figure S8).

Application of dReaMGE in natural product research

The use of exogenous promoters to drive native BGCs is a powerful approach to genome mining and production improvement, and can also avoid interference with complex regulatory networks in the host (48,62). However, BGCs often involve multiple transcription units or operons so a single promoter replacement may not be sufficient to activate a silent BGC or bypass endogenous regulatory circuits (63). Multiplex genome engineering to achieve multiple-promoter replacement and/or combinatorial engineering will simplify the challenges involved in the activation of silent BGCs, deep mining and yield improvement.

The *glb* BGC in DSM 7029 produces the proteasome inhibitor glidobactin A and its analogs (glidobactin B-I and luminmycin A–E) (64). *glb* consists of eight genes (*glbA-glbH*) (Supplementary Table S4) (65), and *glbC* and *glbF* are assigned to encode the nonribosomal peptide-synthetase (NRPS) modules responsible for the macrolactam core structure of glidobactin A. *glbB* encodes a lysine 4-hydroxylase that is responsible for the C4 hydroxylation of L-lysine which is the rate-limiting process of glidobactin A biosynthesis (66). *glbB* and *glbC-glbF* are in different transcription units. Using dReaMGE, simultaneous replacements of *glbB* and the *glbC-glbF* promoters yielded the expected single and double combinations (7029 P_{apra}*glbB*, 7029 P_{apra}*glbC* and 7029 P_{apra}*glbB*-P_{apra}*glbC*; Figure 6A and Supplementary Figure S9A, B). The double mutant promoter strain produced four novel derivatives, luminmycin F to I (Figure 6B,C). Compounds **1** and **2** were isolated and characterized based on mass spectrometry and NMR analysis, while compounds **3** and **4** were characterized based on comparative analysis of HRMS/MS spectra due to a low yield (Figure 6C and Supplementary Figures S10-S24). The fatty acid in **1**–**3** was a tetradecadienoic acid, unique from the dodecadienoic acids Iuminmycin E, luminmycin A and luminmycin B. The clear fragment ions *m/z* 272.14 and *m/z* 464.31 in the MS/MS frag-

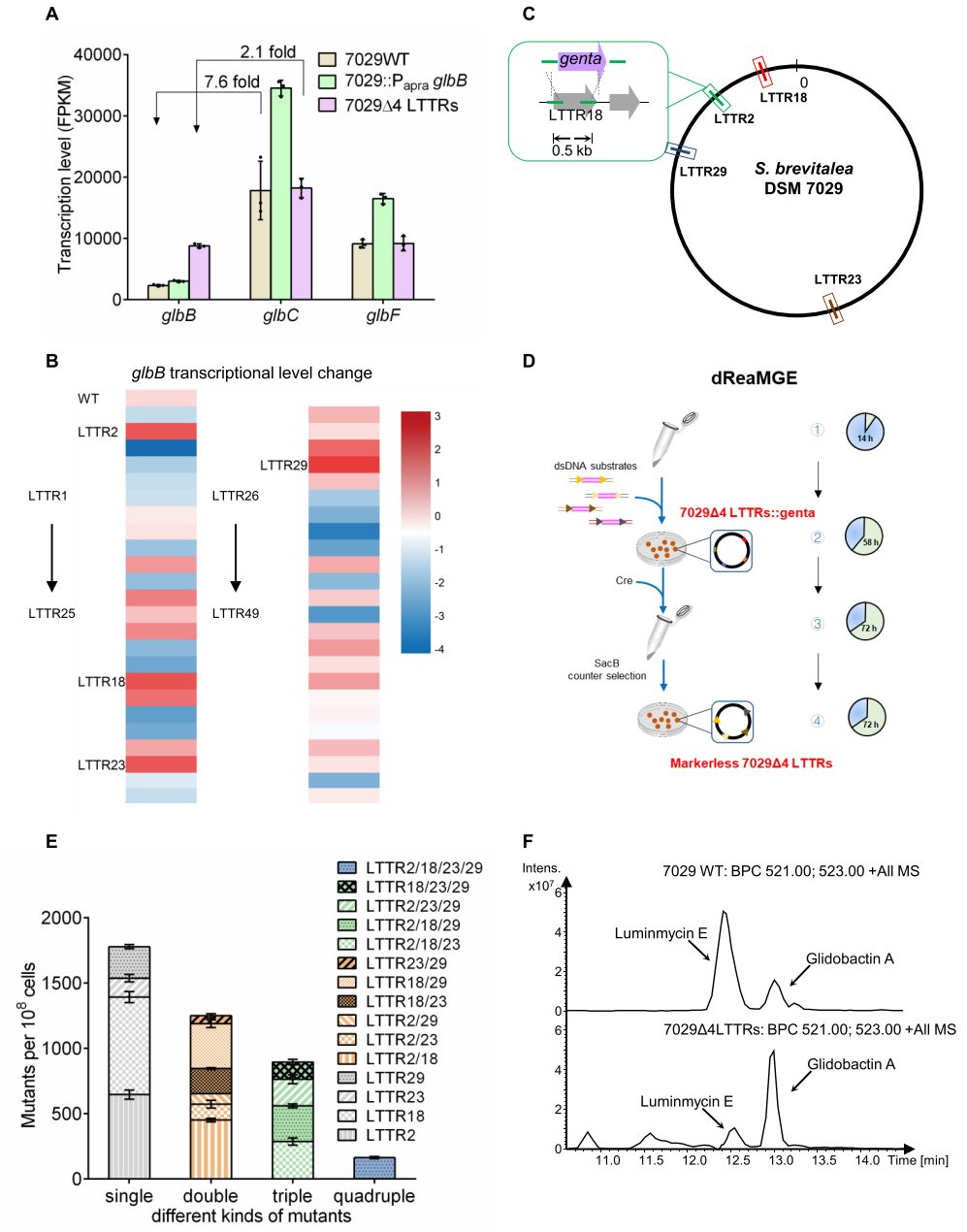

Figure 7. Multiplex analysis of *glb* transcription. (**A**) Comparison of *glbB*, *glbC* and *glbF* mRNA levels in DSM 7029, DSM 7029::P_{apra}*glbB* and DSM 7029Δ4LTTRs::genta strains. (**B**) The effect of 49 single LTTR knockouts on *glbB* mRNA expression presented in color code of log2 fold change compared with the DSM 7029 wild type strain. (**C**) Schematic of the four chosen LTTR replacements. (**D**) Flow diagram of the simultaneous four-LTTR knockout experiment with Cre recombination and sacB counterselection steps. (**E**) Frequencies of the four LTTR mutant combinations generated in DSM 7029 (pBBR1-Rha-Redγ-Redαβ7029-kan). The experiment was repeated 3 times, and 96 recombinants were picked for colony PCR detection each time. (**F**) LC–MS analysis (BPC 521.00; 523.00 + All MS) of extracts from the DSM 7029 wild type strain (7029 WT) and 7029Δ4 LTTRs showed improved glidobactin A yield in the quadruple LTTR knockout strain.

mentation of **4** compared with **1** suggest the existence of an N-dodecadienoyl-threonine-arginine fragment (Supplementary Figure S24, Supplementary Table S12 and S13). Among these four novel derivatives, only the cyclic luminmycin G (**2**) showed weak antitumor activity against human breast cancer cell line MDA-MB-231 (IC_{50} = 10.98 μM), while it was harmless to the human hepatic cell line LO2 (IC_{50} > 400 μM) (Supplementary Table S14). The possible action mode of luminmycin G may involve the α,β-unsaturated carbonyl moiety located in the 12-membered macrolactam ring that could target the N-terminal Thr1-OH active site within the proteasome through Michael-type 1,4-addition (65,66). However the activity of luminmycin G is significantly weaker than glidobactin A, which either relates to the length of the fatty acid chain or the absence of the γ- hydroxyl located in the lysine residue (65,66).

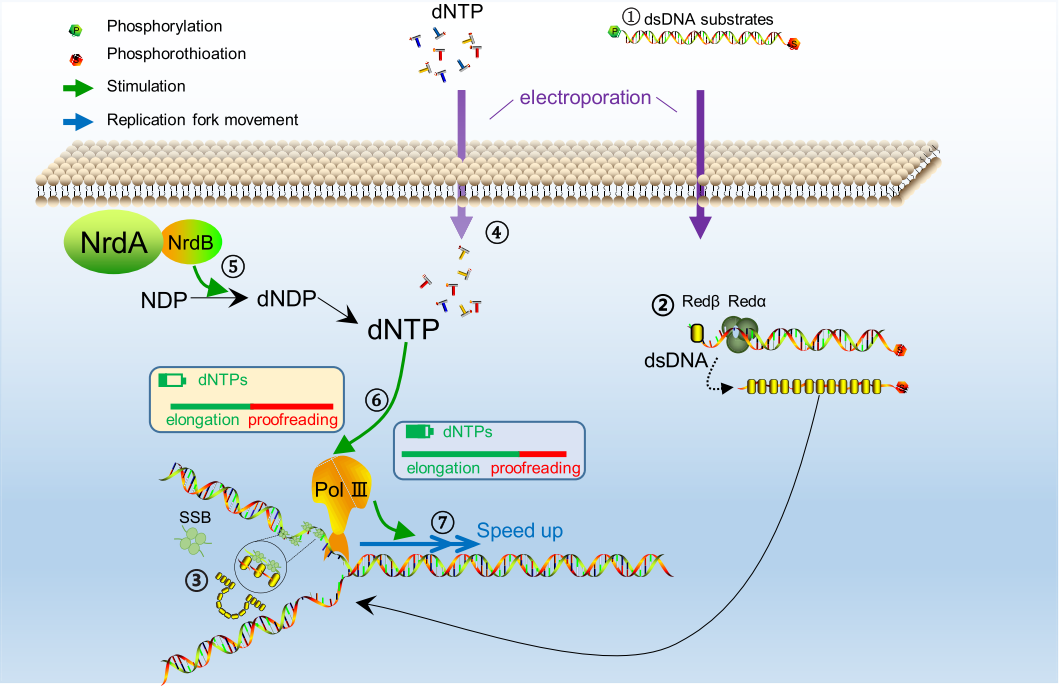

Figure 8. Proposal to explain improved Red recombineering promoted by RNR overexpression and dNTP. ① The dsDNA substrates are electroporated into the host strains. ② The dsDNA substrates digested to ssDNA by Redα while loading Redβ. ③ On the lagging strand template at the replication fork, the Redβ-ssDNA filament displaces SSB protein and the HAs anneal to complementary regions. ④ dNTP levels are elevated during recovery from electroporation. ⑤ RNR overexpression enhances the reduction of NDP to dNDP. ⑥ Increased intracellular dNTP pools shift Pol III to a 'more elongation/less proofreading' mode. ⑦ The 'more elongation/less proofreading' mode of Pol III accelerates DNA chain elongation, leading to accelerated fork movement and increased recombineering efficiency.

Multiplex analysis of glbB and glbC-glbF transcription

Despite the promoter replacements, the yield of glidobactin A was not improved. To tackle the problem in a different way, we sought to understand the transcriptional basis of *glb* BGC expression. First, we used quantitative RT-PCR (qRT-PCR) and found that the transcriptional level of the *glbB* gene was significantly lower than that of *glbC* and *glbF* in the DSM 7029 wild type strain (Figure 7A). Promoter replacement in the 7029 P_{apra}*glbB* strain had little impact on *glbB* expression (Figure 7A). We then established a panel of 49 single lysR transcriptional regulator (LTTR) knockout mutants. Thereby we identified several LTTRs that affected the transcription or stability of *glbB* mRNA (Figure 7B and Supplementary Table S10). To elevate *glbB* expression, we used dReaMGE to combine knockouts of the four LTTRs that each presented the largest individual impact on *glbB* mRNA expression (LTTR2-AAW51_4987, LTTR18-AAW51_5436, LTTR23-AAW51_2727 and LTTR29-AAW51_4579). The quadruple mutation, 7029Δ4LTTR::genta, and the other double and triple combinations (Figure 7C), were obtained in 3 days (14 h for competent cell culture and dsDNA substrate preparation, 2 h for induction and electroporation, 4 h for recovery, 48 h for incubation and 4 h for colony PCR evaluation; Figure 7D). Four percent (4%) of analyzed gentamycin resistant colonies were quadruple 7029Δ4LTTRs::genta (Figure 7E and Supplementary Figure S9C). The level of the *glbB* mRNA in 7029Δ4LTTR was markedly elevated over DSM7029 or DSM7029P_{apra}*glbB* (Figure 7A) and LC–MS analysis showed that the yield of glidobactin A was four times higher (Figure 7F and Supplementary Figure S9D).

DISCUSSION AND CONCLUSION

The application of recombineering to multiplex genome engineering in bacteria forged a new path for the intentional genetic manipulation of living systems (1–4). Using oligonucleotide pools, the remarkable capacity of the lambda phage SSAP, Redβ, has been employed to direct multiplex mutagenesis of the *E. coli* genome. To include dsDNA substrates in the repertoire of multiplex prokaryotic genome recombineering, here we identified five factors that collectively deliver useful frequencies of multiplex mutagenesis; (i) extended recovery time; (ii) lower recovery temperature; (iii) the use of asymmetrically phosphorothioated dsDNA substrates; (iv) the use of only one selectable antibiotic resistance gene; (v) increased dNTP availability. Of these, increased dNTP availability is the most intriguing.

DNA replication in *E. coli* is usually slower than possible to allow more time for the correction of errors, because the supply of dNTPs is limiting (57). We explored the idea that increased replication speed may promote multiplex dsDNA recombineering by elevating expression of RNR (ribonucleotide reductase), which is the enzyme that controls the rate limiting step in dNTP production (56). The decisive success of this experiment encouraged an experi-

ment to simply add dNTPs to the recovery solution after electroporation (Figure 8). This also significantly boosted dsDNA multiplex recombineering. However, the idea that increased replication speed leads to increased frequencies of multiplex dsDNA recombineering is not supported by the advantage delivered by lowering the recovery temperature, which logically should reduce the speed of replication. Also, the counterintuitive finding that use of one antibiotic selectable gene is better than co-selection for two is reminiscent of CoMAGE, where the identification of unselectable oligonucleotide integration is enhanced by selection for a co-transformed selectable oligonucleotide (7,8). Both these unexpected advantages suggest that multiplex recombineering exploits an unusual coincidence. Because recombineering occurs during replication fork progress (28,29), it is likely that this coincidence relates to an unusual composition of, or event at, the replication fork. Potentially elevated dNTP levels, combined with lower recovery temperature and longer recovery times favors the occurrence of the unusual events at the replication fork that promote recombineering.

Because recombineering is based on homologous recombination by infiltration of the replication fork rather than repair of double strand breaks, it is distinct from CRISPR, which promotes HR by DSBs. These two paradigms, HR by replication fork invasion or DSBR, are now the two major applications of precision genome engineering. A third paradigm has been recently described involving CRISPR-assisted site directed transposition (41).

Previously we and others demonstrated that transposition can insert large DNA stretches, thereby overturning the long held belief that transposons could move only small cargoes (67–71). Whether the advantages of transposition can be harvested using CRISPR-assisted site directed transposition remains to be established but progress is promising (42). The future of genome engineering, which will likely differ for prokaryotes and eukaryotes, now involves evaluating the applied merits of (a) recombineering, which does not rely on site directed DNA strand cutting; (b) CRISPR, which promotes HR by site directed cleavage; and (c) site directed transposition.

By achieving, rapidly, various multiplex tasks in diverse bacteria without disturbance of the mismatch repair system or enhancement of the spontaneous mutation rates, dReaMGE expands the repertoire of prokaryotic genome engineering which is a complement to current multiplex genome editing technologies (Supplementary Table S15). To illustrate its' utility, we applied it to manipulate multiple BGCs by inactivation, promoter replacement, and combinatorial modification of transcriptional regulators, as well as substantial genome reduction, for yield improvement of bioactive compounds and discovery of additional derivatives. Multiple rounds of dReaMGE can be used to generate libraries of combinatorically engineered microbes, thereby accelerating directed evolution for the construction of microbial cell factories for elevated yields or the production of novel bioactive compounds.

SUPPLEMENTARY DATA

Supplementary Data are available at NAR Online.

ACKNOWLEDGEMENTS

The authors thank Zhifeng Li, Jingyao Qu, Xiangmei Ren and Haiyan Sui from State Key Laboratory of Microbial Technology of SDU for LC–MS, LC and NMR.
Author contributions: X.B., A.F.S., Y.Z. and X.W. conceived the study; X.B. and Y.Z. supervised the experiments; W.Z. and X.W. performed the experiments; H.Z. carried out structural elucidation of compounds; X.W., W.Z., Q.T., Y.T., A.F.S., Y.Z. and X.B. analyzed data; X.W., X.B., A.F.S. and W.Z. wrote the manuscript with the input from all authors.

FUNDING

National Key R&D Program of China [2021YFC2100500, 2019YFA0905700, 2019YFA0904000]; National Natural Science Foundation of China [32001059, 32070060]; Shandong Provincial Natural Science Foundation, China [ZR2019JQ11]; China Postdoctoral Science Foundation [2019M652373, 2020T130374]; 111 project [B16030]; Youth Interdisciplinary Innovative Research Group [2020QNQT009] of SDU; A.F.S. was funded by the Deutsche Forschungsgemeinschaft [STE 903/6-1]. Funding for open access charge: National Key R&D Program of China; National Natural Science Foundation of China; Shandong Provincial Natural Science Foundation, China.
Conflict of interest statement. None declared.

REFERENCES

1. Csorgo,B., Nyerges,A. and Pal,C. (2020) Targeted mutagenesis of multiple chromosomal regions in microbes. *Curr. Opin. Microbiol.*, **57**, 22–30.
2. Song,C.W., Lee,J. and Lee,S.Y. (2015) Genome engineering and gene expression control for bacterial strain development. *Biotechnol. J.*, **10**, 56–68.
3. Cao,M., Tran,V.G. and Zhao,H. (2020) Unlocking nature's biosynthetic potential by directed genome evolution. *Curr Opin Biotech.*, **66**, 95–104.
4. Wang,H.H., Isaacs,F.J., Carr,P.A., Sun,Z.Z., Xu,G., Forest,C.R. and Church,G.M. (2009) Programming cells by multiplex genome engineering and accelerated evolution. *Nature*, **460**, 894–898.
5. Warner,J.R., Reeder,P.J., Karimpour-Fard,A., Woodruff,L.B.A. and Gill,R.T. (2010) Rapid profiling of a microbial genome using mixtures of barcoded oligonucleotides. *Nat. Biotechnol.*, **28**, 856–862.
6. Isaacs,F.J., Carr,P.A., Wang,H.H., Lajoie,M.J., Sterling,B., Kraal,L., Tolonen,A.C., Gianoulis,T.A., Goodman,D.B., Reppas,N.B. *et al.* (2011) Precise manipulation of chromosomes in vivo enables genome-wide codon replacement. *Science*, **333**, 348–353.
7. Carr,P.A., Wang,H.H., Sterling,B., Isaacs,F.J., Lajoie,M.J., Xu,G., Church,G.M. and Jacobson,J.M. (2012) Enhanced multiplex genome engineering through co-operative oligonucleotide co-selection. *Nucleic Acids Res.*, **40**, e132.
8. Wang,H.H., Kim,H., Cong,L., Jeong,J., Bang,D. and Church,G.M. (2012) Genome-scale promoter engineering by coselection MAGE. *Nat. Methods*, **9**, 591–593.
9. Nyerges,A., Csorgo,B., Nagy,I., Balint,B., Bihari,P., Lazar,V., Apjok,G., Umenhoffer,K., Bogos,B., Posfai,G. *et al.* (2016) A highly precise and portable genome engineering method allows comparison of mutational effects across bacterial species. *Proc. Natl. Acad. Sci. U.S.A.*, **113**, 2502–2507.
10. Cobb,R.E., Wang,Y.J. and Zhao,H.M. (2015) High-efficiency multiplex genome editing of *Streptomyces* species using an engineered CRISPR/Cas system. *ACS Synth. Biol.*, **4**, 723–728.
11. Jiang,W.Y., Bikard,D., Cox,D., Zhang,F. and Marraffini,L.A. (2013) RNA-guided editing of bacterial genomes using CRISPR-Cas systems. *Nat. Biotechnol.*, **31**, 233–239.

12. Ronda,C., Pedersen,L.E., Sommer,M.O.A. and Nielsen,A.T. (2016) CRMAGE: CRISPR optimized MAGE Recombineering. *Sci. Rep.-UK*, **6**, 19452.
13. Garst,A.D., Bassalo,M.C., Pines,G., Lynch,S.A., Halweg-Edwards,A.L., Liu,R., Liang,L., Wang,Z., Zeitoun,R., Alexander,W.G. *et al.* (2017) Genome-wide mapping of mutations at single-nucleotide resolution for protein, metabolic and genome engineering. *Nat. Biotechnol.*, **35**, 48–55.
14. Reisch,C.R. and Prather,K.L.J. (2017) Scarless Cas9 Assisted Recombineering (no-SCAR) in *Escherichia coli*, an easy-to-use system for genome editing. *Curr. Protoc. Mol. Biol.*, **117**, 31.8.1–31.8.20.
15. Jiang,Y., Chen,B., Duan,C.L., Sun,B.B., Yang,J.J. and Yang,S. (2015) Multigene editing in the *Escherichia coli* genome via the CRISPR-Cas9 system. *Appl. Environ. Microb.*, **81**, 2506–2514.
16. Zhang,Y., Buchholz,F., Muyrers,J.P.P. and Stewart,A.F. (1998) A new logic for DNA engineering using recombination in Escherichia coli. *Nat. Genet.*, **20**, 123–128.
17. Muyrers,J.P.P., Zhang,Y.M., Testa,G. and Stewart,A.F. (1999) Rapid modification of bacterial artificial chromosomes by ET-recombination. *Nucleic Acids Res.*, **27**, 1555–1557.
18. Zhang,Y.M., Muyrers,J.P.P., Testa,G. and Stewart,A.F. (2000) DNA cloning by homologous recombination in Escherichia coli. *Nat. Biotechnol.*, **18**, 1314–1317.
19. Murphy,K.C., Campellone,K.G. and Poteete,A.R. (2000) PCR-mediated gene replacement in Escherichia coli. *Gene*, **246**, 321–330.
20. Yu,D.G., Ellis,H.M., Lee,E.C., Jenkins,N.A., Copeland,N.G. and Court,D.L. (2000) An efficient recombination system for chromosome engineering in Escherichia coli. *Proc. Natl. Acad. Sci. U.S.A.*, **97**, 5978–5983.
21. Datsenko,K.A. and Wanner,B.L. (2000) One-step inactivation of chromosomal genes in *Escherichia coli* K-12 using PCR products. *Proc. Natl. Acad. Sci. U.S.A.*, **97**, 6640–6645.
22. Fu,J., Bian,X., Hu,S., Wang,H., Huang,F., Seibert,P.M., Plaza,A., Xia,L., Muller,R., Stewart,A.F. *et al.* (2012) Full-length RecE enhances linear-linear homologous recombination and facilitates direct cloning for bioprospecting. *Nat. Biotechnol.*, **30**, 440–446.
23. Zhang,Y.M., Muyrers,J.P.P., Rientjes,J. and Stewart,F. (2003) Phage annealing proteins promote oligonucleotide-directed mutagenesis in Escherichia coli and mouse ES cells. *BMC Mol. Biol.*, **4**, 1.
24. Erler,A., Wegmann,S., Elie-Caille,C., Bradshaw,C.R., Maresca,M., Seidel,R., Habermann,B., Muller,D.J. and Stewart,A.F. (2009) Conformational adaptability of red beta during DNA annealing and implications for its structural relationship with Rad52. *J. Mol. Biol.*, **391**, 586–598.
25. Aparicio,T., Nyerges,A., Martinez-Garcia,E. and de Lorenzo,V. (2020) High-efficiency multi-site genomic editing of *Pseudomonas putida* through thermoinducible ssDNA recombineering. *iScience*, **23**, 100946.
26. Nyerges,A., Csorgo,B., Draskovits,G., Kintses,B., Szili,P., Ferenc,G., Revesz,T., Aria,E., Nagy,I., Balint,B. *et al.* (2018) Directed evolution of multiple genomic loci allows the prediction of antibiotic resistance. *Proc. Natl. Acad. Sci. U.S.A.*, **115**, E5726–E5735.
27. Reif,B., Ashbrook,S.E., Emsley,L. and Hong,M. (2021) Recombineering and MAGE. *Nat. Rev. Methods Primers*, **1**, 8.
28. Maresca,M., Erler,A., Fu,J., Friedrich,A., Zhang,Y.M. and Stewart,A.F. (2010) Single-stranded heteroduplex intermediates in lambda Red homologous recombination. *BMC Mol. Biol.*, **11**, 54.
29. Mosberg,J.A., Lajoie,M.J. and Church,G.M. (2010) Lambda red recombineering in *Escherichia coli* occurs through a fully single-stranded intermediate. *Genetics*, **186**, 791–799.
30. Ellis,H.M., Yu,D.G., DiTizio,T. and Court,D.L. (2001) High efficiency mutagenesis, repair, and engineering of chromosomal DNA using single-stranded oligonucleotides. *Proc. Natl. Acad. Sci. U.S.A.*, **98**, 6742–6746.
31. Muyrers,J.P.P., Zhang,Y.M., Buchholz,F. and Stewart,A.F. (2000) RecE/RecT and Red alpha/Red beta initiate double-stranded break repair by specifically interacting with their respective partners. *Gene Dev.*, **14**, 1971–1982.
32. Subramaniam,S., Erler,A., Fu,J., Kranz,A., Tang,J., Gopalswamy,M., Ramakrishnan,S., Keller,A., Grundmeier,G., Muller,D. *et al.* (2016) DNA annealing by Red beta is insufficient for homologous recombination and the additional requirements involve intra- and inter-molecular interactions. *Sci. Rep.-UK*, **6**, 34525.
33. Smith,C.E. and Bell,C.E. (2016) Domain structure of the redo single-strand annealing protein: the C-terminal domain is required for fine-tuning DNA-binding properties, interaction with the exonuclease partner, and recombination in vivo. *J. Mol. Biol.*, **428**, 561–578.
34. Caldwell,B.J. and Bell,C.E. (2019) Structure and mechanism of the Red recombination system of bacteriophage lambda. *Prog. Biophys. Mol. Biol.*, **147**, 33–46.
35. Brewster,J.L. and Tolun,G. (2020) Half a century of bacteriophage lambda recombinase: In vitro studies of lambda exonuclease and Red-beta annealase. *IUBMB Life*, **72**, 1622–1633.
36. Jinek,M., Chylinski,K., Fonfara,I., Hauer,M., Doudna,J.A. and Charpentier,E. (2012) A programmable dual-RNA-guided DNA endonuclease in adaptive bacterial immunity. *Science*, **337**, 816–821.
37. Gasiunas,G., Barrangou,R., Horvath,P. and Siksnys,V. (2012) Cas9-crRNA ribonucleoprotein complex mediates specific DNA cleavage for adaptive immunity in bacteria. *Proc. Natl Acad. Sci. U.S.A.*, **109**, E2579–E2586.
38. Doudna,J.A. and Charpentier,E. (2014) The new frontier of genome engineering with CRISPR-Cas9. *Science*, **346**, 1077.
39. Sharda,M., Badrinarayanan,A. and Seshasayee,A.S.N. (2020) Evolutionary and comparative analysis of bacterial nonhomologous end joining repair. *Genome Biol. Evol.*, **12**, 2450–2466.
40. Wang,Y., Cheng,H., Liu,Y., Liu,Y., Wen,X., Zhang,K., Ni,X., Gao,N., Fan,L., Zhang,Z. *et al.* (2021) In-situ generation of large numbers of genetic combinations for metabolic reprogramming via CRISPR-guided base editing. *Nat. Commun.*, **12**, 678.
41. Klompe,S.E., Vo,P.L.H., Halpin-Healy,T.S. and Sternberg,S.H. (2019) Transposon-encoded CRISPR-Cas systems direct RNA-guided DNA integration. *Nature*, **571**, 219–225.
42. Vo,P.L.H., Ronda,C., Klompe,S.E., Chen,E.E., Acree,C., Wang,H.H. and Sternberg,S.H. (2021) CRISPR RNA-guided integrases for high-efficiency, multiplexed bacterial genome engineering. *Nat. Biotechnol.*, **39**, 480–489.
43. Yao,L., Cengic,I., Anfelt,J. and Hudson,E.P. (2016) Multiple gene repression in cyanobacteria using CRISPRi. *ACS Synth Biol*, **5**, 207–212.
44. Zhao,Y.W., Li,L., Zheng,G.S., Jiang,W.H., Deng,Z.X., Wang,Z.J. and Lu,Y.H. (2018) CRISPR/dCas9-mediated multiplex gene repression in *Streptomyces*. *Biotechnol. J.*, **13**, e1800121.
45. Datta,S., Costantino,N., Zhou,X. and Court,D.L. (2008) Identification and analysis of recombineering functions from Gram-negative and Gram-positive bacteria and their phages. *Proc. Natl Acad. Sci. U.S.A.*, **105**, 1626–1631.
46. Filsinger,G.T., Wannier,T.M., Pedersen,F.B., Lutz,I.D., Zhang,J., Stork,D.A., Debnath,A., Gozzi,K., Kuchwara,H., Volf,V. *et al.* (2021) Characterizing the portability of phage-encoded homologous recombination proteins. *Nat. Chem. Biol.*, **17**, 394–402.
47. Yin,J., Zhu,H., Xia,L., Ding,X., Hoffmann,T., Hoffmann,M., Bian,X., Muller,R., Fu,J., Stewart,A.F. *et al.* (2015) A new recombineering system for Photorhabdus and Xenorhabdus. *Nucleic Acids Res.*, **43**, e36.
48. Wang,X., Zhou,H.B., Chen,H.N., Jing,X.S., Zheng,W.T., Li,R.J., Sun,T., Liu,J.Q., Fu,J., Huo,L.J. *et al.* (2018) Discovery of recombinases enables genome mining of cryptic biosynthetic gene clusters in Burkholderiales species. *Proc. Natl. Acad. Sci. U.S.A.*, **115**, E4255–E4263.
49. Zheng,W., Wang,X., Zhou,H., Zhang,Y., Li,A. and Bian,X. (2020) Establishment of recombineering genome editing system in *Paraburkholderia megapolitana* empowers activation of silent biosynthetic gene clusters. *Microb. Biotechnol.*, **13**, 397–405.
50. Yin,J., Zheng,W., Gao,Y., Jiang,C., Shi,H., Diao,X., Li,S., Chen,H., Wang,H., Li,R. *et al.* (2019) Single-stranded DNA-binding protein and exogenous RecBCD inhibitors enhance phage-derived homologous recombination in *Pseudomonas*. *iScience*, **14**, 1–14.
51. Lee,G. and Saito,I. (1998) Role of nucleotide sequences of loxP spacer region in Cre-mediated recombination. *Gene*, **216**, 55–65.
52. Wang,H.L., Li,Z., Jia,R.N., Hou,Y., Yin,J., Bian,X.Y., Li,A.Y., Muller,R., Stewart,A.F., Fu,J. *et al.* (2016) RecET direct cloning and Red alpha beta recombineering of biosynthetic gene clusters, large operons or single genes for heterologous expression. *Nat. Protoc.*, **11**, 1175–1190.
53. Tang,B., Yu,Y.C., Liang,J.H., Zhang,Y.M., Bian,X.Y., Zhi,X.Y. and Ding,X.M. (2019) Reclassification of '*Polyangium brachysporum*'

DSM 7029 as *Schlegelella brevitalea* sp. nov. *Int. J. Syst. Evol. Micr.*, **69**, 2877–2883.
54. Mao,D., Bushin,L.B., Moon,K., Wu,Y. and Seyedsayamdost,M.R. (2017) Discovery of scmR as a global regulator of secondary metabolism and virulence in Burkholderia thailandensis E264. *Proc. Natl Acad. Sci. U.S.A.*, **114**, E2920–E2928.
55. Mosmann,T. (1983) Rapid colorimetric assay for cellular growth and survival: application to proliferation and cytotoxicity assays. *J. Immunol. Methods*, **65**, 55–63.
56. Kolberg,M., Strand,K.R., Graff,P. and Andersson,K.K. (2004) Structure, function, and mechanism of ribonucleotide reductases. *Biochim. Biophys. Acta*, **1699**, 1–34.
57. Wheeler,L.J., Rajagopal,I. and Mathews,C.K. (2005) Stimulation of mutagenesis by proportional deoxyribonucleoside triphosphate accumulation in *Escherichia coli*. *DNA Repair (Amst.)*, **4**, 1450–1456.
58. Odsbu,I., Morigen and Skarstad,K. (2009) A reduction in ribonucleotide reductase activity slows down the chromosome replication fork but does not change its localization. *PLoS One*, **4**, e7617.
59. Gon,S., Napolitano,R., Rocha,W., Coulon,S. and Fuchs,R.P. (2011) Increase in dNTP pool size during the DNA damage response plays a key role in spontaneous and induced-mutagenesis in Escherichia coli. *Proc. Natl. Acad. Sci. U.S.A.*, **108**, 19311–19316.
60. Si,F., Li,D., Cox,S.E., Sauls,J.T., Azizi,O., Sou,C., Schwartz,A.B., Erickstad,M.J., Jun,Y., Li,X. *et al.* (2017) Invariance of initiation mass and predictability of cell size in *Escherichia coli*. *Curr. Biol.*, **27**, 1278–1287.
61. Pham,T.M., Tan,K.W., Sakumura,Y., Okumura,K., Maki,H. and Akiyama,M.T. (2013) A single-molecule approach to DNA replication in *Escherichia coli* cells demonstrated that DNA polymerase III is a major determinant of fork speed. *Mol. Microbiol.*, **90**, 584–596.
62. Song,C., Luan,J., Cui,Q., Duan,Q., Li,Z., Gao,Y., Li,R., Li,A., Shen,Y., Li,Y. *et al.* (2019) Enhanced heterologous spinosad production from a 79-kb synthetic multioperon assembly. *ACS Synth Biol*, **8**, 137–147.
63. Bian,X.Y., Plaza,A., Zhang,Y.M. and Muller,R. (2012) Luminmycins A-C, cryptic natural products from photorhabdus luminescens identified by heterologous expression in *Escherichia coli*. *J. Nat. Prod.*, **75**, 1652–1655.
64. Schellenberg,B., Bigler,L. and Dudler,R. (2007) Identification of genes involved in the biosynthesis of the cytotoxic compound glidobactin from a soil bacterium. *Environ. Microbiol.*, **9**, 1640–1650.
65. Bian,X.Y., Huang,F., Wang,H.L., Klefisch,T., Muller,R. and Zhang,Y.M. (2014) Heterologous production of glidobactins/luminmycins in *Escherichia coli* nissle containing the glidobactin biosynthetic gene cluster from Burkholderia DSM7029. *ChemBioChem*, **15**, 2221–2224.
66. Amatuni,A. and Renata,H. (2019) Identification of a lysine 4-hydroxylase from the glidobactin biosynthesis and evaluation of its biocatalytic potential. *Org. Biomol. Chem.*, **17**, 1736–1739.
67. Fu,J., Wenzel,S.C., Perlova,O., Wang,J., Gross,F., Tang,Z., Yin,Y., Stewart,A.F., Muller,R. and Zhang,Y. (2008) Efficient transfer of two large secondary metabolite pathway gene clusters into heterologous hosts by transposition. *Nucleic Acids Res.*, **36**, e113.
68. Suster,M.L., Sumiyama,K. and Kawakami,K. (2009) Transposon-mediated BAC transgenesis in zebrafish and mice. *BMC Genomics*, **10**, 477.
69. Li,MA, Turner,DJ, Ning,Z, Yusa,K, Liang,Q, Eckert,S, Rad,L, Fitzgerald,TW, Craig,NL and Bradley,A. (2011) Mobilization of giant piggyBac transposons in the mouse genome. *Nucleic Acids Res.*, **39**, e148.
70. Rostovskaya,M., Fu,J., Obst,M., Baer,I., Weidlich,S., Wang,H., Smith,A.J., Anastassiadis,K. and Stewart,A.F. (2012) Transposon-mediated BAC transgenesis in human ES cells. *Nucleic Acids Res.*, **40**, e150.
71. Rostovskaya,M., Naumann,R., Fu,J., Obst,M., Mueller,D., Stewart,A.F. and Anastassiadis,K. (2013) Transposon mediated BAC transgenesis via pronuclear injection of mouse zygotes. *Genesis*, **51**, 135–141.